PRDW
Consulting Port and Coastal Engineers

GRANGER BAY VISION

Wave and Hydrodynamic Modelling Study

REV.C

07 November 2025

V&A WATEFRONT
Cape Town, South Africa

PRDW
Consulting Port and Coastal Engineers

GRANGER BAY VISION

Wave and Hydrodynamic Modelling Study

S2105-07-RP-CE-001-RC

07 November 2025

REV.	TYPE	DATE	EXECUTED	CHECK	APPROVED	CLIENT	DESCRIPTION / COMMENTS
A	A	14/06/2023	SRW	SAL	SAL		Draft Report
B	C	30/08/2023	SRW	SAL	SAL		Updated based on comments from V&A
C	C	07/11/2025	SRW	SAL			Updated Sections 3.4 and 4.

TYPE OF ISSUE: (A) Draft (B) To bid or proposal (C) For Approval (D) Approved (E) Void

V&A WATEFRONT
Cape Town, South Africa

PRDW
5th Floor, Nedbank Building, Clock Tower Precinct, Victoria & Alfred Waterfront
Cape Town, South Africa | PO Box 50023, Waterfront 8002
T: +27 21 418 3830
www.prdw.com

Cape Town, South Africa
Santiago, Chile
Perth, Australia
Seattle, USA
Vitoria, Brazil
Panama City, Panama

PRDW
Consulting Port and Coastal Engineers

CONTENTS

Page N°

TABLE OF CONTENTS I
1. INTRODUCTION 1
1.1 Project background 1
1.2 Objectives 1
1.3 Layouts 2
1.4 Methodology 3
1.5 Limitations 3
2. MODELLING 4
2.1 Hydrodynamic model 4
2.1.1 Description 4
2.1.2 Setup 4
2.1.2.1 Mesh and bathymetry 4
2.1.2.2 Wind 8
2.1.2.3 Boundary conditions 11
2.1.2.4 Model settings 11
2.1.3 Calibration 11
2.1.3.1 Water levels 11
2.1.3.2 Currents 12
2.1.3.3 Seawater temperature 12
2.1.4 Cases modelled 13
2.2 Phase-resolving wave model 13
2.2.1 Description 13
2.2.2 Setup 14
2.2.2.1 Bathymetry and mesh 14
2.2.2.2 Model inputs 17
2.2.3 Calibration 17
2.2.4 Critical bed shear stress 19
2.2.5 Cases modelled 23
3. RESULTS 25
3.1 Current speed and direction 25
3.2 Flushing of water and seawater temperature 30
3.3 Wave heights 35
3.4 Accumulation of mud 40
4. SUMMARY 45
5. REFERENCES 46

TABLES

Page N°

Table 2-1: Global hindcast models used for the model boundary conditions. 11
Table 2-2: Model inputs at 15:00 for the 13 July 2020 storm. 17
Table 2-3: Wave parameters in -20 m MSL. 24

FIGURES

Page N°

Figure 1-1: Site Location. 1
Figure 1-2: Baseline layout (top) and the new “cascade” development layout (bottom). 2

Figure 1-3: Concept of the “cascade” development layout. 3
Figure 2-1: Model bathymetry for the baseline layout. 5
Figure 2-2: Model mesh for the baseline layout. 6
Figure 2-3: Detailed bathymetry and mesh for the baseline layout. 7
Figure 2-4: Detailed bathymetry and mesh for the development layout. 8
Figure 2-5: Snapshots illustrating the high spatial variability in the 4 km resolution modelled winds around Cape Town for two wind directions (grey lines show topography at 100 m intervals). 9
Figure 2-6: Time series of modelled compared to measured winds at Cape Town International, Cape Point and Koeberg. 10
Figure 2-7: Time series comparison of modelled water levels to predicted tides at the Port of Cape Town. 11
Figure 2-8: Time series comparison of measured and modelled current speed and direction near the Green Point outfall. 12
Figure 2-9: Summer/autumn: Time series of measured and modelled seawater temperatures. 13
Figure 2-10: Overview of bathymetry for whole domain (baseline layout). 14
Figure 2-11: Overview of mesh for whole domain (baseline layout). 15
Figure 2-12: Detailed bathymetry for baseline layout. 15
Figure 2-13: Detailed mesh for baseline layout. 16
Figure 2-14: Detailed bathymetry for new development layout. 16
Figure 2-15: Detailed mesh for new development layout. 17
Figure 2-16: Instantaneous modelled surface elevation of an overtopping event during the 13 July 2020 storm. 18
Figure 2-17: Overtopping of rock revetment at approximately 15:00 on 13 July 2020. Photo credit: Stephen Luger. 19
Figure 2-18: Overtopping in front of Grand Africa Café on 13 July 2020 (exact time unknown). Photo credit: Anton Holtzhausen. 19
Figure 2-19: Percentage fines obtained from a number of historical sediment sampling campaigns. 20
Figure 2-20: Correlation of the percentage fines measured in grab samples of the seabed sediment and the 95th percentile modelled bed shear stress. 21
Figure 2-21: Modelled bed shear stresses during 1-year return period storm. 22
Figure 2-22: High-resolution bathymetric survey of the Waterclub (Tritan Survey, 2021) 22
Figure 2-23: High-resolution bathymetric survey of Granger Bay (Underwater Surveys, 2022). 23
Figure 2-24: Time series of H_{m0} at -20 m MSL for a representative year with 1-month summer, 1-month winter and 1-year return period significant storm wave heights indicated. 24
Figure 3-1: Instantaneous depth-averaged current speed during a south-easterly wind event for the baseline (top) and development (bottom) layouts. 26
Figure 3-2: Instantaneous depth-averaged current speed during a north-westerly wind event for the baseline (top) and development (bottom) layouts. 27
Figure 3-3: Maximum (99th percentile) depth-averaged current speed for the baseline (top) and development (bottom) layouts for the summer/autumn case. 28
Figure 3-4: Maximum (99th percentile) depth-averaged current speed for the baseline (top) and development (bottom) layouts for the winter/spring case. 29
Figure 3-5: Depth-averaged residual currents for the baseline (top) and development (bottom) layouts for the summer/autumn case. 31
Figure 3-6: Depth-averaged residual currents for the baseline (top) and development (bottom) layouts for the winter/spring case. 32

Figure 3-7: Maximum (99th percentile) surface seawater temperature for the baseline (top) and development (bottom) layouts for the summer/autumn case. 33
Figure 3-8: Maximum (99th percentile) surface seawater temperature for the baseline (top) and development (bottom) layouts for the winter/spring case. 34
Figure 3-9: instantaneous surface elevations for baseline (top) and development (bottom) layouts for the 1-year return period. 36
Figure 3-10: Total H_{m0} for baseline (top) and development (bottom) layouts for the 1-year return period. 37
Figure 3-11: Total H_{m0} for baseline (top) and development (bottom) layouts for the 1-month return period in summer. 38
Figure 3-12: Total H_{m0} for baseline (top) and development (bottom) layouts for the 1-month return period in winter. 39
Figure 3-13: Wave-induced bed shear stress for baseline (top) and development (bottom) layouts for the 1-year return period storm event. 41
Figure 3-14: Wave-induced bed shear stress for baseline (top) and development (bottom) layouts for the 1-month return period storm event in summer. 42
Figure 3-15: Wave-induced bed shear stress for baseline (top) and development (bottom) layouts for the 1-month return period storm event in winter. 43

1. INTRODUCTION

1.1 Project background

The proposed Granger Bay development is located between the Western dolos revetment and the Granger Bay Small Craft Harbour, also known as the Waterclub, as shown in Figure 1-1.

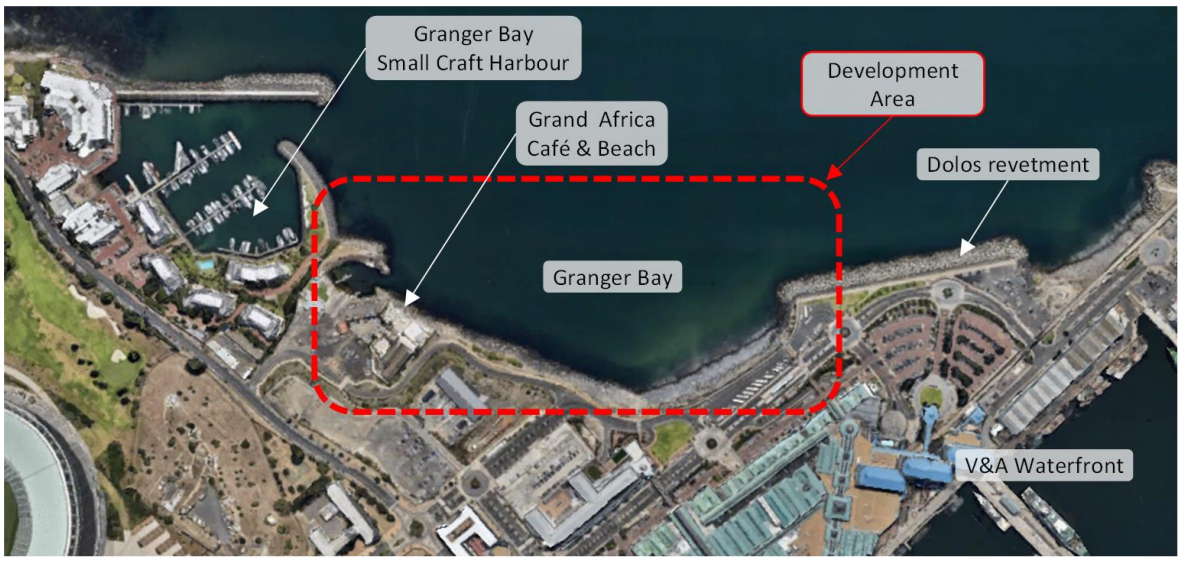

Figure 1-1: Site Location.

PRDW have been appointed by the V&A Waterfront to undertake a numerical modelling study of the proposed development to determine the changes that the proposed development will have on the marine environment.

1.2 Objectives

The objectives of this study are to estimate the changes that the proposed development will have on the following physical parameters:

- Current speed and direction;
- Flushing of water and seawater temperatures within the new basin;
- Wave heights;
- Accumulation of mud on the seabed (the existing seabed in Granger Bay is generally sandy because during large wave events any mud that is deposited during calm periods is resuspended, but it is possible that the new development will reduce the waves sufficiently to reduce the resuspension of mud and thus increase the percentage of mud on the seabed, with associated changes in marine ecology).

These results will provide inputs to the marine ecology study.

1.3 Layouts

Two layouts will be assessed:

1. The existing situation as shown in Figure 1-2, referred to as the baseline layout.
2. The new "cascade" layout of the development as shown in Figure 1-2, referred to in this report as the development layout. The cascade layout consists of the construction of two new breakwaters extending off the Oceana breakwater and the existing dolos revetment, reclaiming land and constructing a new revetment between the existing dolos revetment and the breakwater. The crest level of the proposed development is +5.5 m MSL. A 3D impression of the cascade layout can be seen in Figure 1-3.

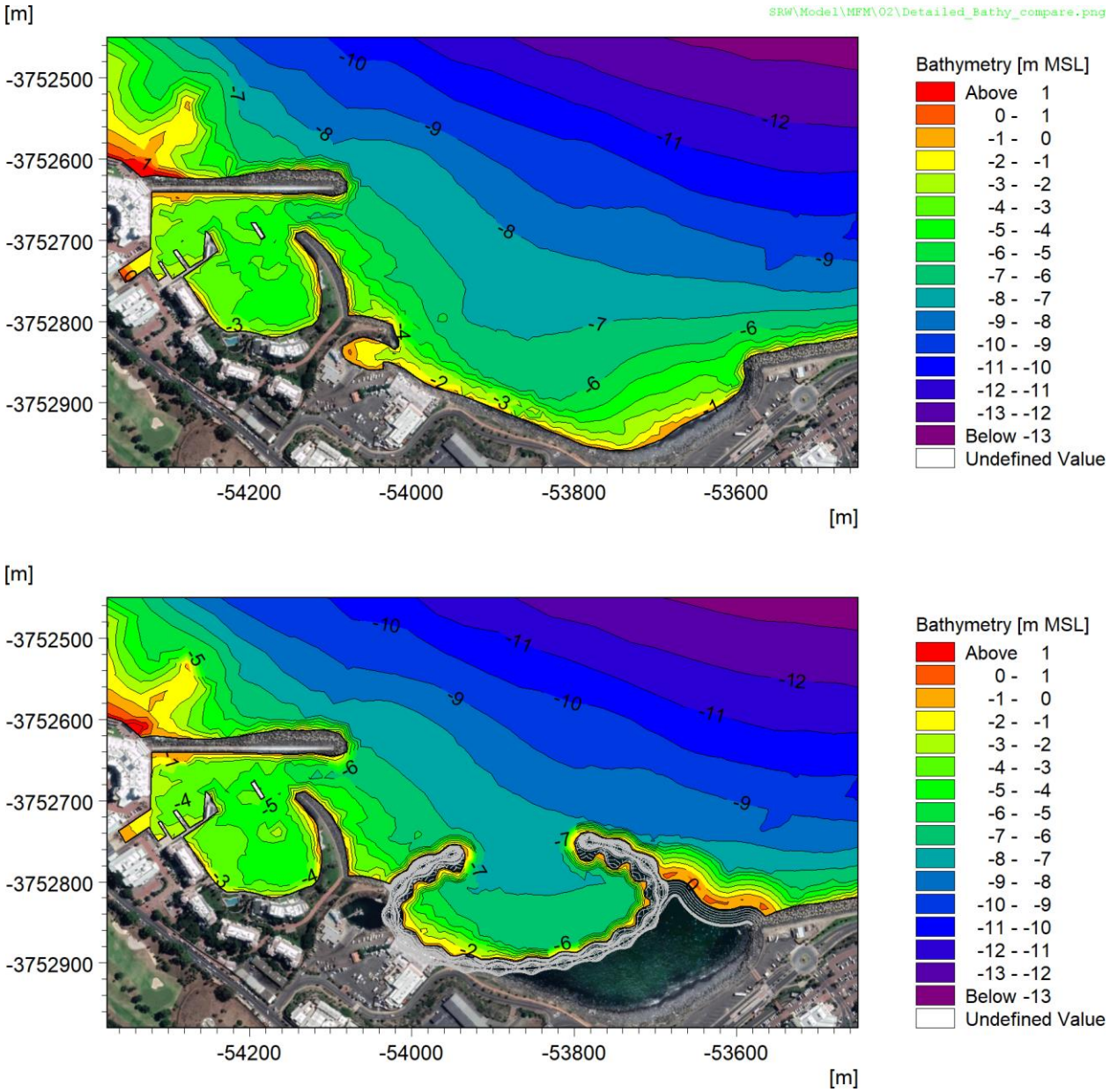

Figure 1-2: Baseline layout (top) and the new "cascade" development layout (bottom).

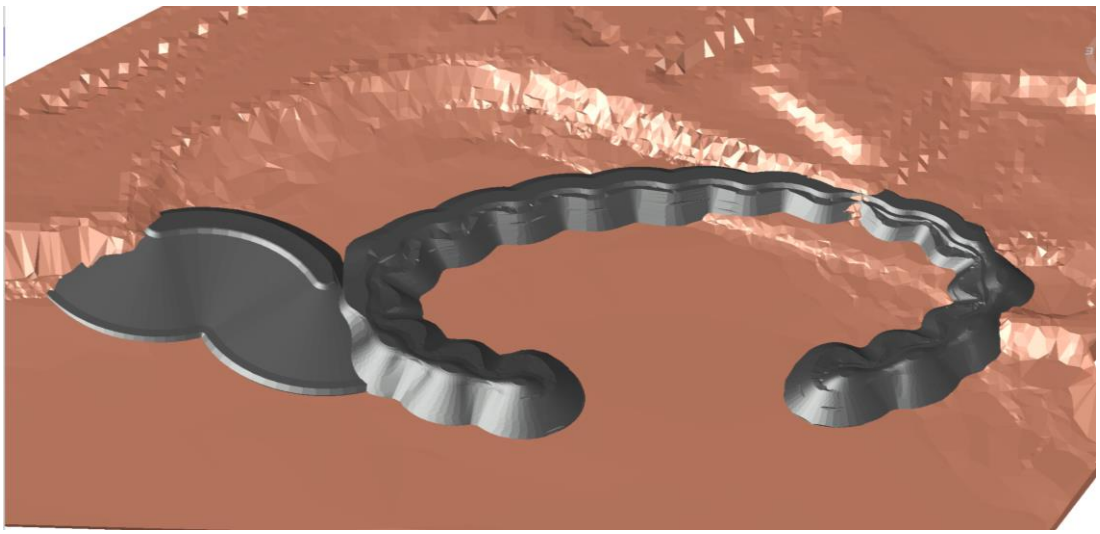

Figure 1-3: Concept of the "cascade" development layout.

1.4 Methodology

A 3D hydrodynamic numerical model will be used to simulate the currents, water levels, seawater temperature and salinity including forcing due to wind, tides, upwelling and regional currents. The model will be run for 6 weeks in summer/autumn and 6 weeks in winter/spring. The model has previously been calibrated against measurements. The outputs will be the following for both layouts for both summer/autumn and winter/spring:

- The maximum depth-averaged current speed for each layout.
- The residual depth-averaged current speed for each layout (this is the vector averaged current and indicates the flushing of the basin).
- The maximum surface seawater temperature for each layout.

A wave refraction numerical model will be used to simulate the wave transformation from deepwater to a depth of 20 m offshore of Granger Bay for one year. A 3D phase-resolving wave numerical model will then be used to simulate the combined short and long waves for each layout for a number of wave conditions, i.e. the 1-month return period storm in summer, 1-month return period storm in winter and 1-year return period storm. The outputs will be the following:

- Wave height for each layout for each wave condition.
- Combined short and long wave induced bed shear stress for each layout. These shear stresses will be compared to critical shear stresses for mud resuspension, which will allow the spatial and temporal extent of possible mud deposition inside the development to be estimated.

1.5 Limitations

The model outputs will need to be interpreted by the marine ecologists to assess the impact on the marine ecology. Should the marine ecologists assess the impacts due to any of these parameters to be significant, then additional modelling may be required. This may include testing mitigation options such as permeable or slotted breakwaters to improve flushing, redirecting stormwater discharges to outside the development (if applicable), more detailed assessment of mud accumulation, etc. This additional modelling is excluded from the current scope.

2. MODELLING

This section contains technical details of the setup and calibration of the numerical models.

2.1 Hydrodynamic model

2.1.1 Description

The three-dimensional MIKE 3 Flow Flexible Mesh Model was used to model the currents and seawater temperatures. The application of the model is described in the User Manual (DHI, 2023a), while full details of the physical processes being simulated and the numerical solution techniques are described in the Scientific Documentation (DHI, 2023b).

The model is based on the numerical solution of the three-dimensional incompressible Reynolds averaged Navier-Stokes equations invoking the assumptions of Boussinesq and of hydrostatic pressure. The model consists of the continuity, momentum, temperature, salinity and density equations and is closed by a k-ε vertical turbulence closure scheme. Horizontal eddy viscosity is modelled with the Smagorinsky formulation.

The time integration of the shallow water equations and the transport equations is performed using a semi-implicit scheme, where the horizontal terms are treated explicitly and the vertical terms are treated implicitly. In the vertical direction a structured mesh, based on a sigma-coordinate transformation is used, while the geometrical flexibility of the unstructured flexible mesh comprising triangles or quadrangles is utilised in the horizontal plane.

The model includes the following physical phenomena:

- Currents due to tides;
- Currents due to wind stress on the water surface;
- Currents due to density gradients caused by seawater temperature and salinity;
- Coriolis forcing;
- Bottom friction;
- Flooding and drying;
- Heat exchange.

2.1.2 Setup

2.1.2.1 Mesh and bathymetry

The WG19 horizontal coordinate system was used for this study. All spatial plots include x and y axes showing the x and y coordinates in metres in the WG19 system. True north is always pointing upwards. The vertical datum adopted in this study is Mean Sea Level (MSL).

The model mesh comprises triangles with a resolution varying from about 3 km at the offshore boundary to 10 m in the vicinity of the site. The vertical mesh is comprised of twelve sigma layers with equal layer thicknesses.

The model bathymetry has been obtained from the following sources:

- CMAP electronic hydrographic charts (DHI, 2023c),
- Available bathymetric surveys in Table Bay,
- Granger Bay hydrographic survey (Underwater Surveys, 2022).

Figure 2-1 and Figure 2-2 present the model bathymetry and mesh, respectively, for the baseline layout while Figure 2-3 and Figure 2-4 present detail around the site for baseline and development layout.

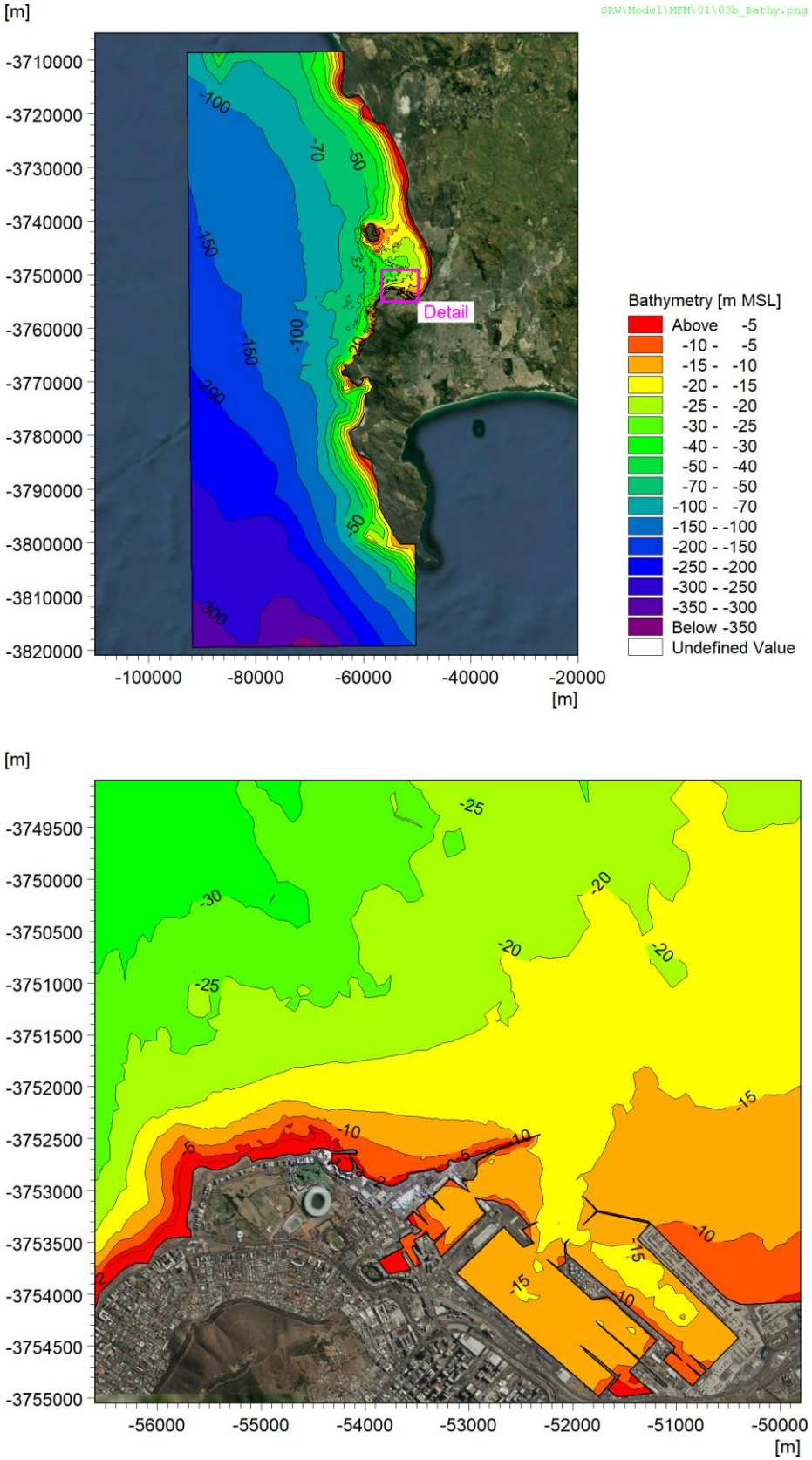

Figure 2-1: Model bathymetry for the baseline layout.

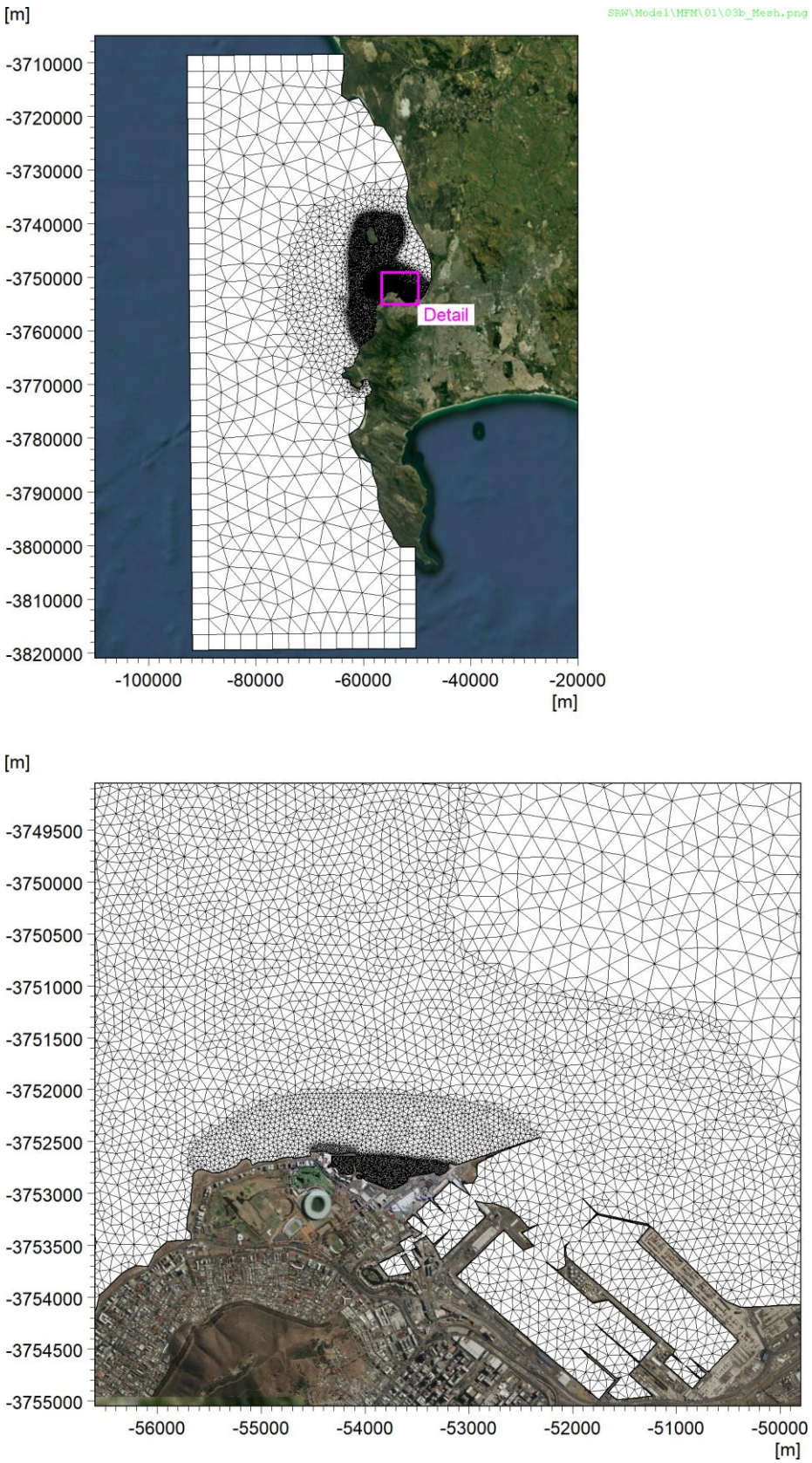

Figure 2-2: Model mesh for the baseline layout.

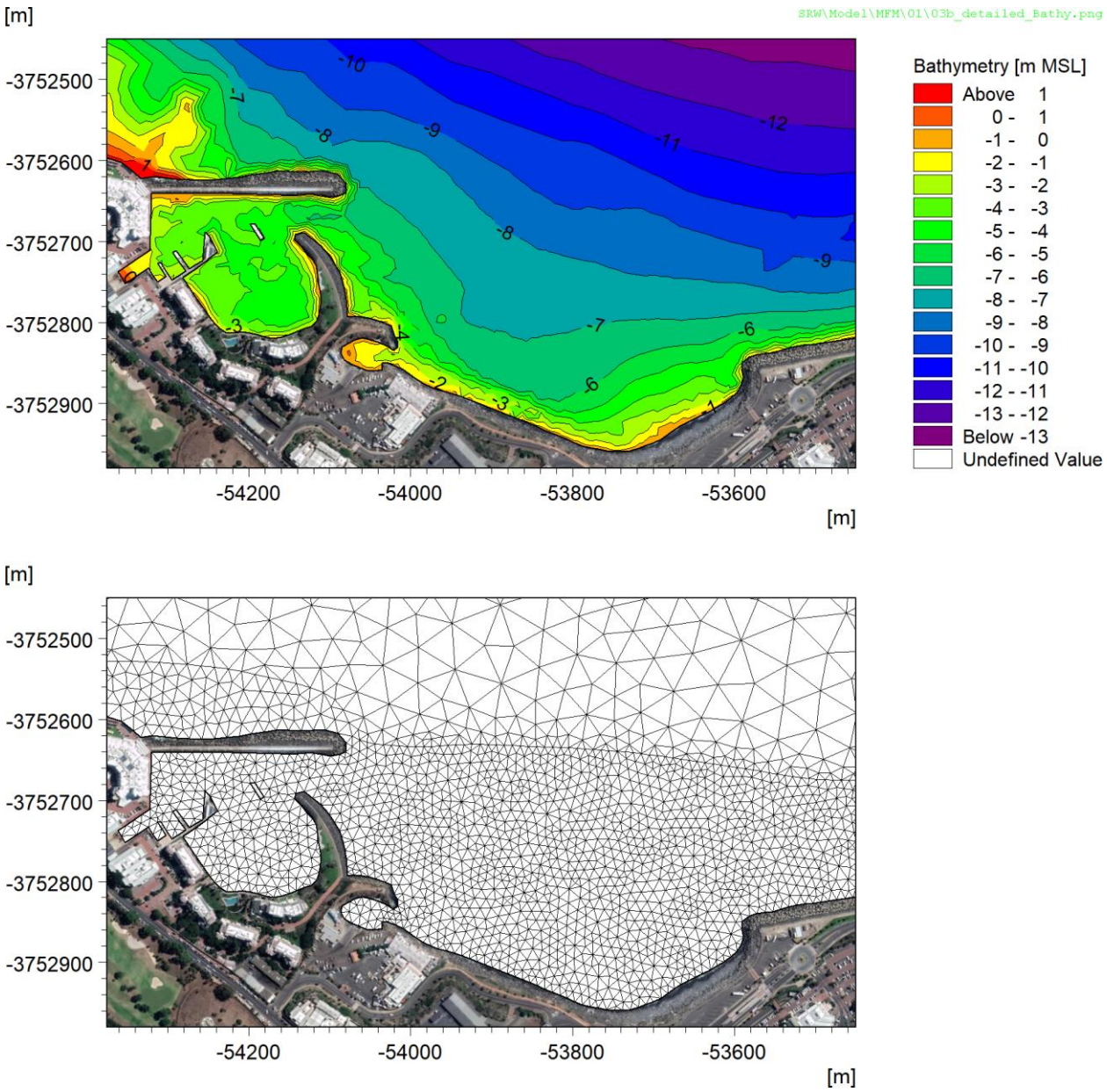

Figure 2-3: Detailed bathymetry and mesh for the baseline layout.

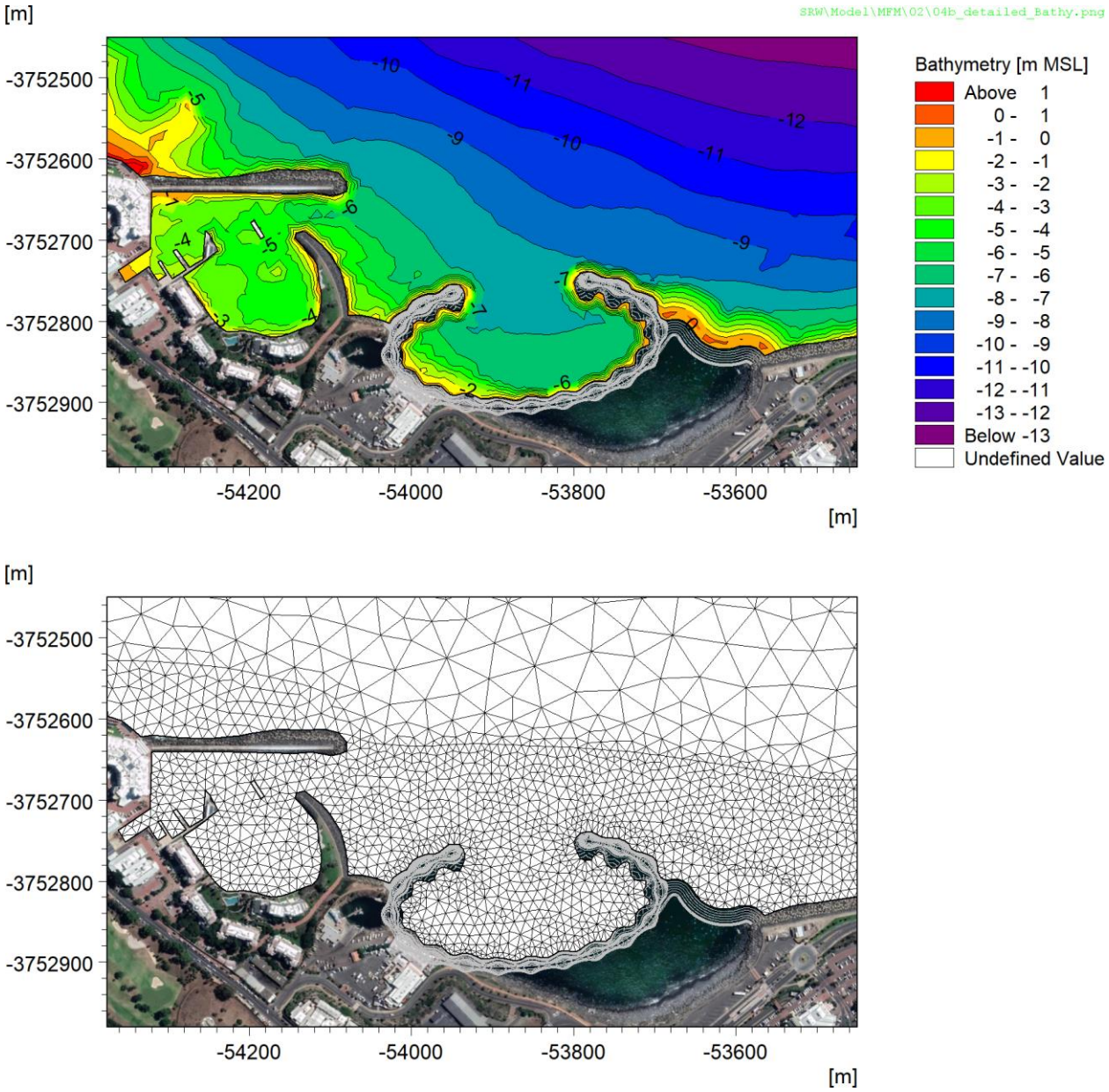

Figure 2-4: Detailed bathymetry and mesh for the development layout.

2.1.2.2 Wind

Wind is an important forcing mechanism for currents, vertical mixing and upwelling. The wind fields near the outfalls are influenced by the surrounding mountains and thus require a high spatial resolution. The Climate System Analysis Group at the University of Cape Town has kindly provided wind data from the Weather Research and Forecasting (WRF) model with a spatial resolution of 4 km and a temporal resolution of 1 hour.

Figure 2-5 shows two snapshots in time illustrating the high spatial variability in the 4 km resolution modelled winds around Cape Town. Figure 2-6 shows a time series comparison between the modelled winds and measured winds at three locations around Cape Town (Cape Town International Airport, Cape Point and Koeberg) for the winter/spring and summer/autumn modelling periods. These results indicate that the WRF modelled winds compare well to the measured winds at three different locations across Cape Town and will thus provide reliable forcing to the hydrodynamic model.

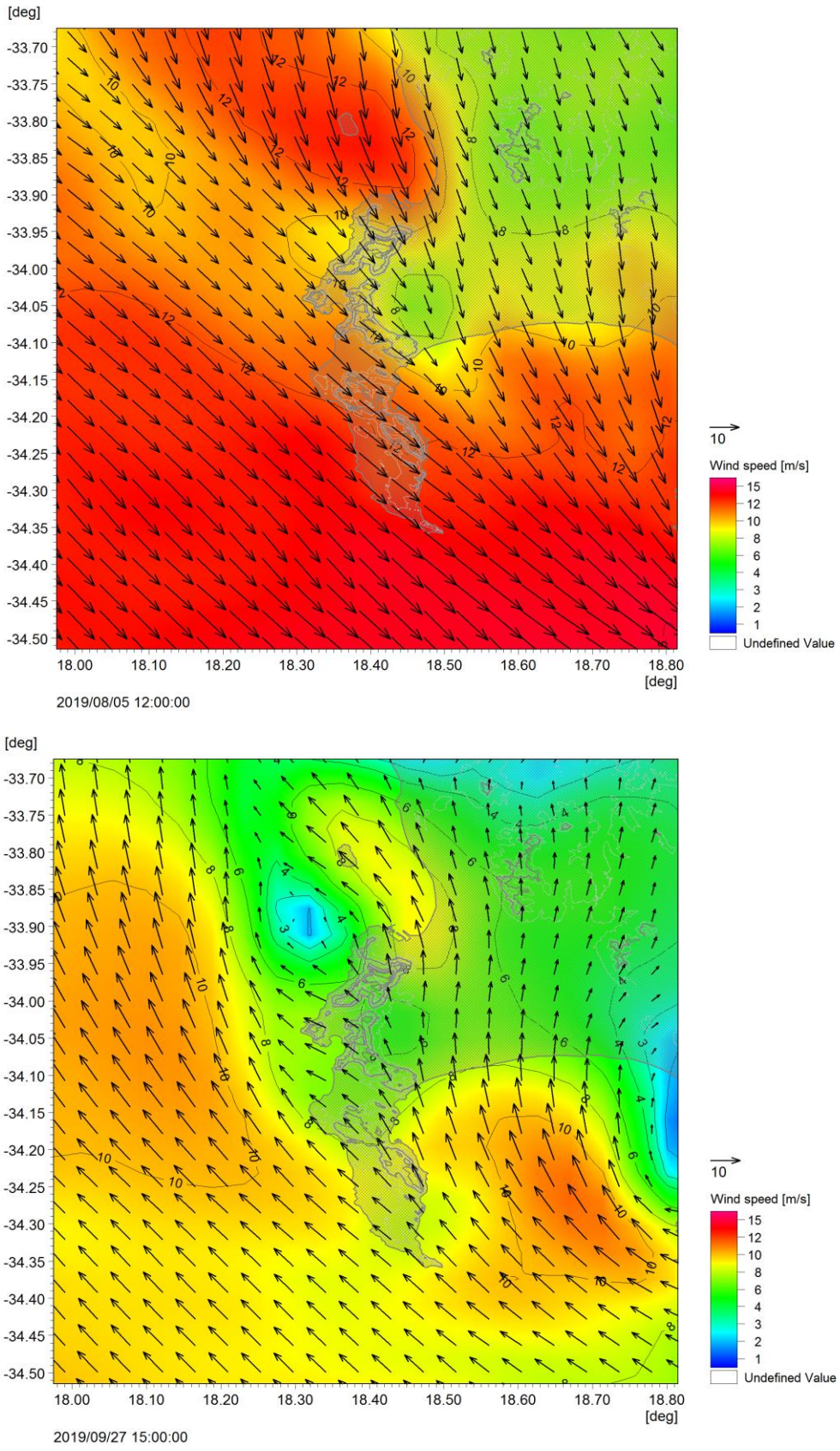

Figure 2-5: Snapshots illustrating the high spatial variability in the 4 km resolution modelled winds around Cape Town for two wind directions (grey lines show topography at 100 m intervals).

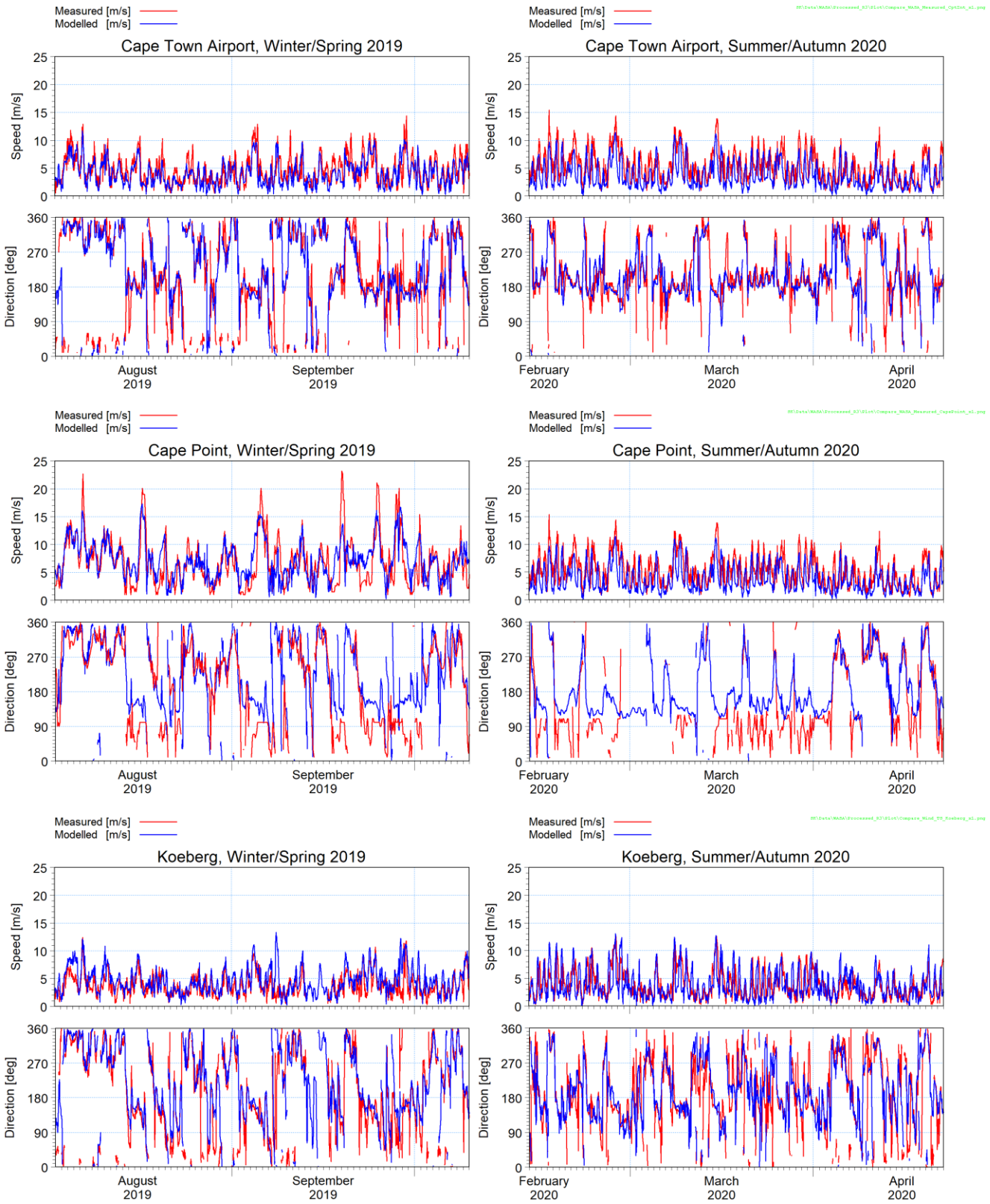

Figure 2-6: Time series of modelled compared to measured winds at Cape Town International, Cape Point and Koeberg.

2.1.2.3 Boundary conditions

The model boundary conditions were extracted from global hindcast models as described in Table 2-1:

Table 2-1: Global hindcast models used for the model boundary conditions.

Model	Parameter	Spatial resolution [°]	Temporal resolution [hrs]
HYbrid Coordinate Ocean Model (HYCOM) global ocean circulation model (HYCOM, 2020).	Non-tidal water levels	0.08	3
	Non-tidal ocean currents		
	Seawater temperature		
	Seawater salinity		
DTU10 (Technical University of Denmark) global tidal model (DTU, 2010).	Predicted tides	0.125	Predicted from constituents.
	Predicted tidal currents	0.25	
European Centre for Medium-Range Weather Forecasts (EMCWF) ERA5 global atmospheric model (ECMWF, 2020).	Air temperature	0.25	1
	Humidity		
	Solar radiation		

2.1.2.4 Model settings

The vertical eddy viscosity was computed using the k-ε vertical turbulence closure scheme, while the vertical eddy dispersion was set to 0.1 times the vertical eddy viscosity. This scaling factor was applied to compensate for additional vertical mixing caused by the use of only 12 vertical layers and the associated smoothing of the vertical density gradients.

The wind friction coefficient and seabed roughness were tuned to physically realistic values which yielded the best agreement between modelled and measured currents at Green Point.

2.1.3 Calibration

The model was calibrated to measured water level, current and seawater temperatures, as described below.

2.1.3.1 Water levels

The predicted tidal levels at the Port of Cape Town were extracted from the MIKE by DHI CMAP Electronic Charts Database (DHI, 2023c). Figure 2-7 presents a time series comparison of modelled water levels to predicted tides at the Port of Cape Town. The comparison shows an excellent comparison in both tidal phase and amplitude.

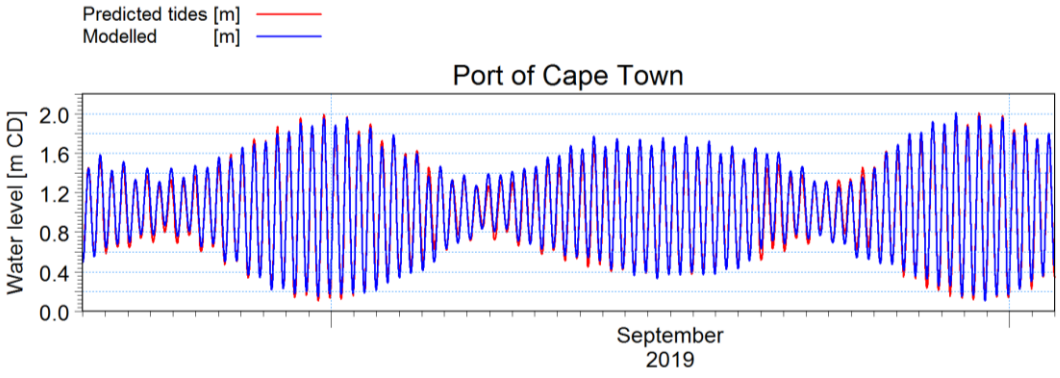

Figure 2-7: Time series comparison of modelled water levels to predicted tides at the Port of Cape Town.

2.1.3.2 Currents

Figure 2-8 presents a time series comparison of the modelled and measured currents near the end of the Green Point outfall. Note that current direction is by convention the direction towards which the current is flowing. Overall, the model reproduces the main features of both the surface and seabed currents and is considered acceptably accurate for the purposes of this study.

Figure 2-8: Time series comparison of measured and modelled current speed and direction near the Green Point outfall.

2.1.3.3 Seawater temperature

The modelled seawater temperatures were compared to measurements near the end of the Green Point outfall as shown in Figure 2-9 . The measured time series shows that the seawater temperatures are complex and vary over a range of time-scales due to upwelling, solar radiation and other dynamic processes. The model is able to predict the mean trend in seabed seawater temperatures including some of the discrete dynamic events. The modelled sub-surface temperatures tend to be overpredicted while the surface temperatures tend to be underpredicted. Despite these limitations the model is considered adequately calibrated for seawater temperature for the purposes of this study.

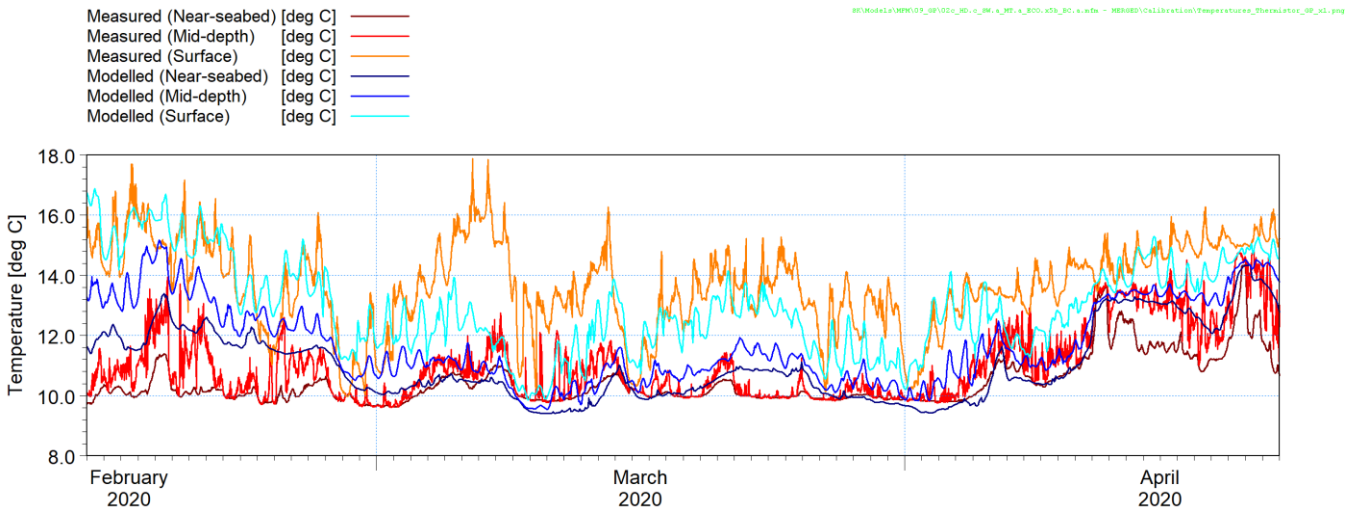

Figure 2-9: Summer/autumn: Time series of measured and modelled seawater temperatures.

2.1.4 Cases modelled

Two cases of six weeks each were modelled for the hydrodynamics. These periods were selected based on the availability of calibration data.

- A summer/autumn period from 14/02/2020 to 27/03/2020.
- A winter/spring period from 01/08/2019 to 12/09/2019.

2.2 Phase-resolving wave model

2.2.1 Description

The MIKE 3 Wave Model FM (M3WFM) was used to simulate the wave heights and wave-induced bed shear stresses.

M3WFM is a phase-resolving wave model based on the 3D Navier-Stokes equations and with the free surface described by a height function. The numerical techniques applied are based on an unstructured (flexible) mesh approach. The application of M3WFM is described in the User Manual (DHI, 2023d), while full details of the physical processes being simulated and the numerical solution techniques are described in the Scientific Documentation (DHI, 2023e). The model validation by DHI is described in the Validation Report (DHI, 2023f). PRDW have also validated the model for wave run-up and overtopping using measured data.

The M3WFM model includes the following processes:

- Wave refraction;
- Wave diffraction;
- Bottom friction;
- Non-linear wave transformation;
- Surf and swash zone hydrodynamics;
- Wave breaking and run-up;
- Wave overtopping;
- Coastal flooding; and
- Wave transmission (and reflection) through porous structures.

The model is based on the numerical solution of the three-dimensional incompressible Reynolds-averaged Navier-Stokes equations. Thus, the model consists of continuity and momentum equations, and it is closed by a k-ε turbulence closure scheme in the vertical and horizontal. The free surface is taken into account using a sigma coordinate transformation approach. The spatial discretization of the governing equations in conserved form is performed using a cell-centred finite volume method. The time integration is performed using a semi-implicit scheme. The vertical convective and diffusion terms are discretized using an implicit scheme to remove the stability limitations associated with the vertical resolution. The remaining terms are discretized using a second-order explicit Runge-Kutta scheme. The projection method is employed for the non-hydrostatic pressure. The interface convective fluxes are calculated using a HLLC approximate Riemann solver. This shock-capturing scheme enables robust and stable simulation of flows involving shocks or discontinuities such as bores and hydraulic jumps. This is essential for modelling of waves in the breaking zone or porous structures. The numerical dissipation accounts for the dissipation in the breaking waves.

2.2.2 Setup

2.2.2.1 Bathymetry and mesh

The model bathymetry has been obtained from the following sources:

- CMAP electronic hydrographic charts (DHI, 2023c),
- Available bathymetric surveys in Table Bay,
- Granger Bay hydrographic survey (Underwater Surveys, 2022).

The flexible mesh comprises triangles with a resolution varying between approximately 6.5 m offshore and approximately 3 m around the study area in Granger Bay.

The model bathymetry and mesh are presented in Figure 2-10 and Figure 2-11 for the whole domain for the baseline layout. Figure 2-12 to Figure 2-15 present detailed bathymetries and meshes for the study area for the baseline layout and the new development layout.

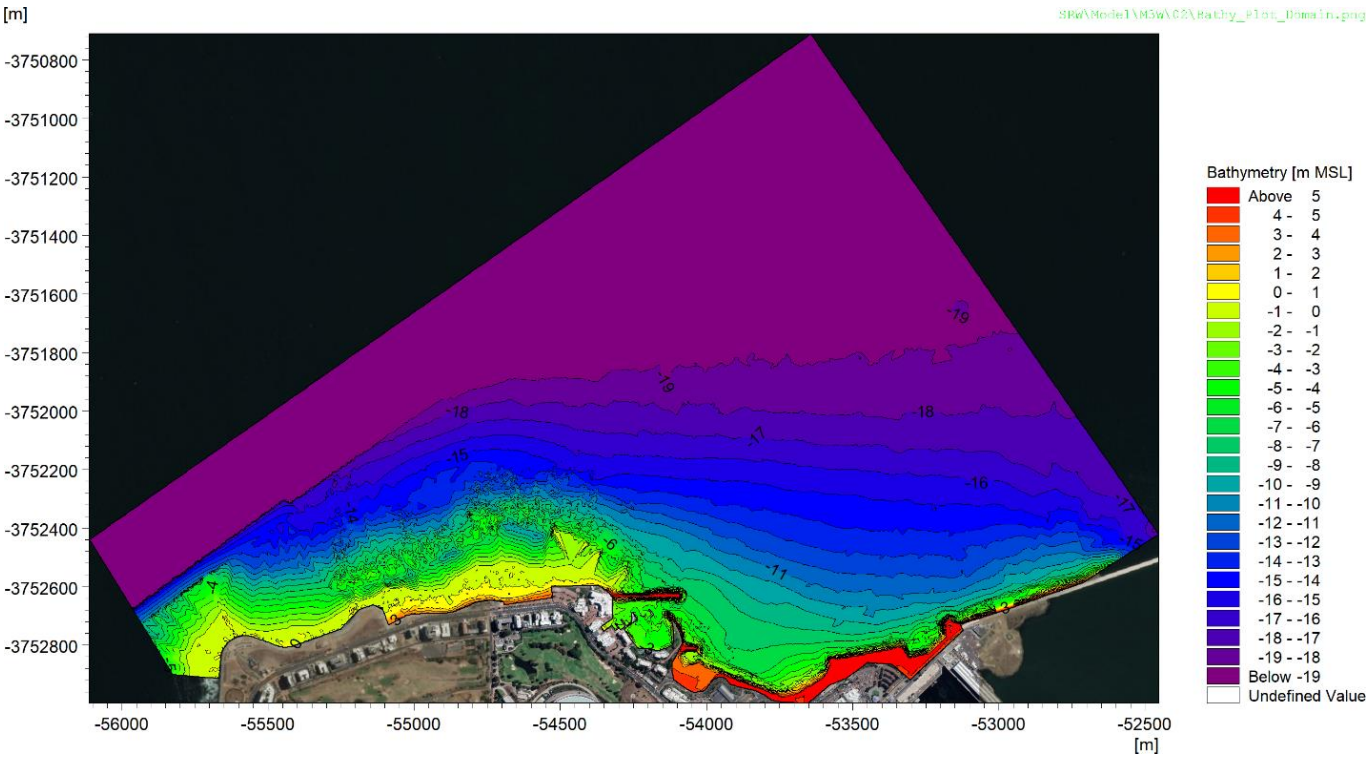

Figure 2-10: Overview of bathymetry for whole domain (baseline layout).

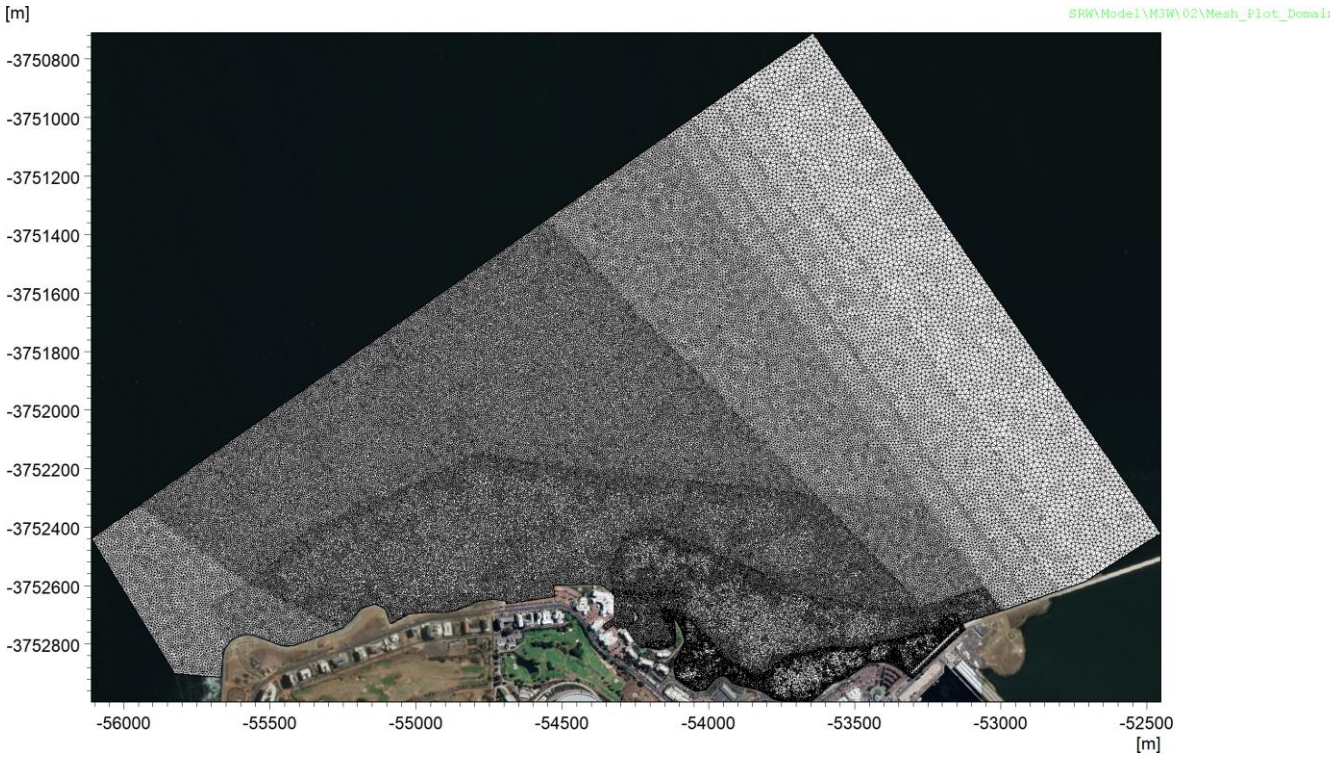

Figure 2-11: Overview of mesh for whole domain (baseline layout).

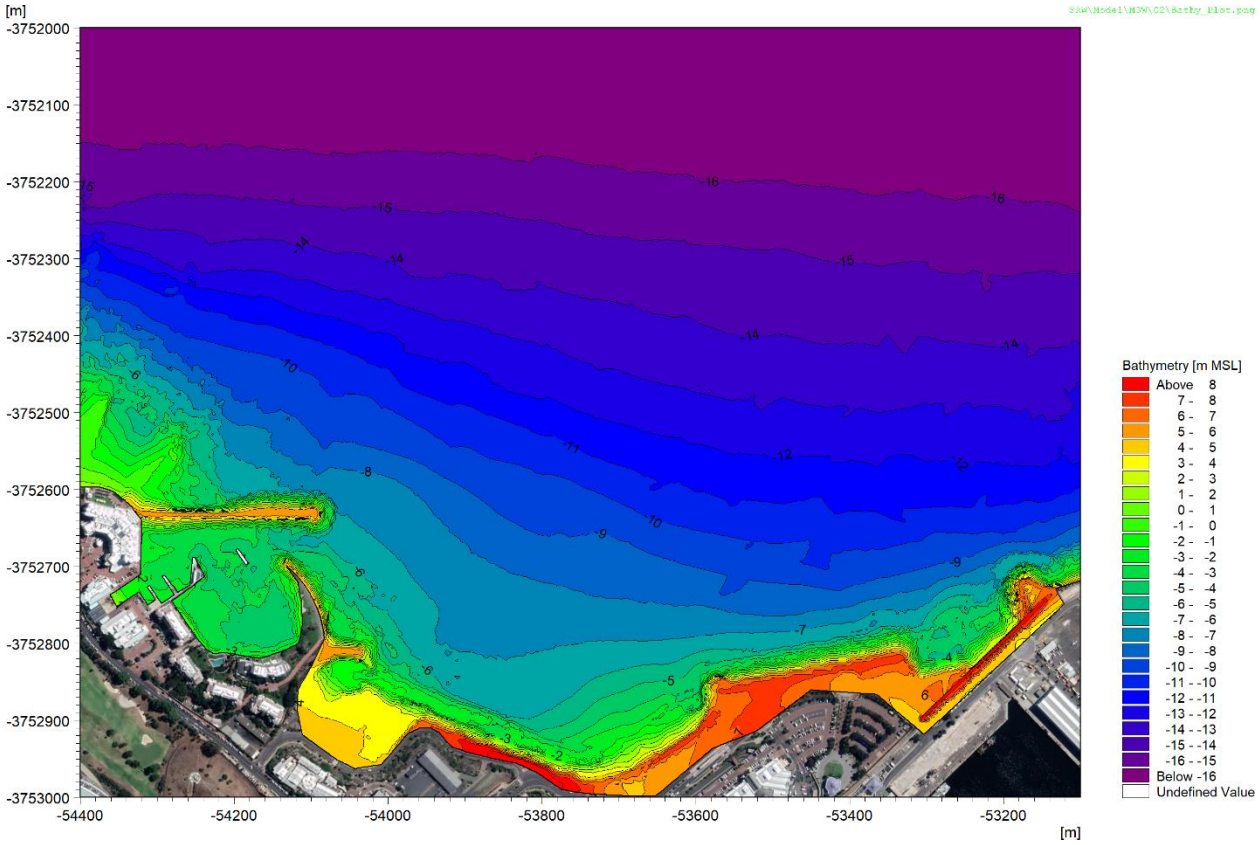

Figure 2-12: Detailed bathymetry for baseline layout.

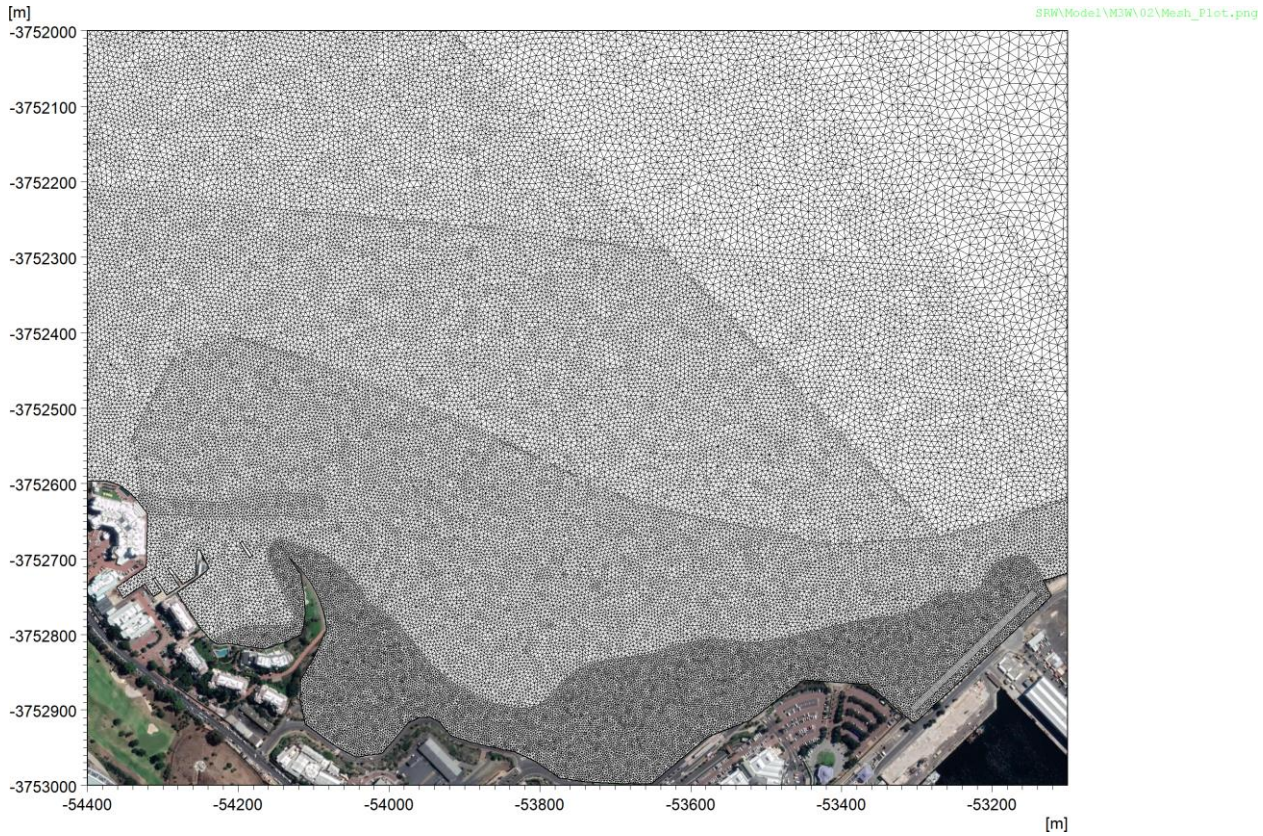

Figure 2-13: Detailed mesh for baseline layout.

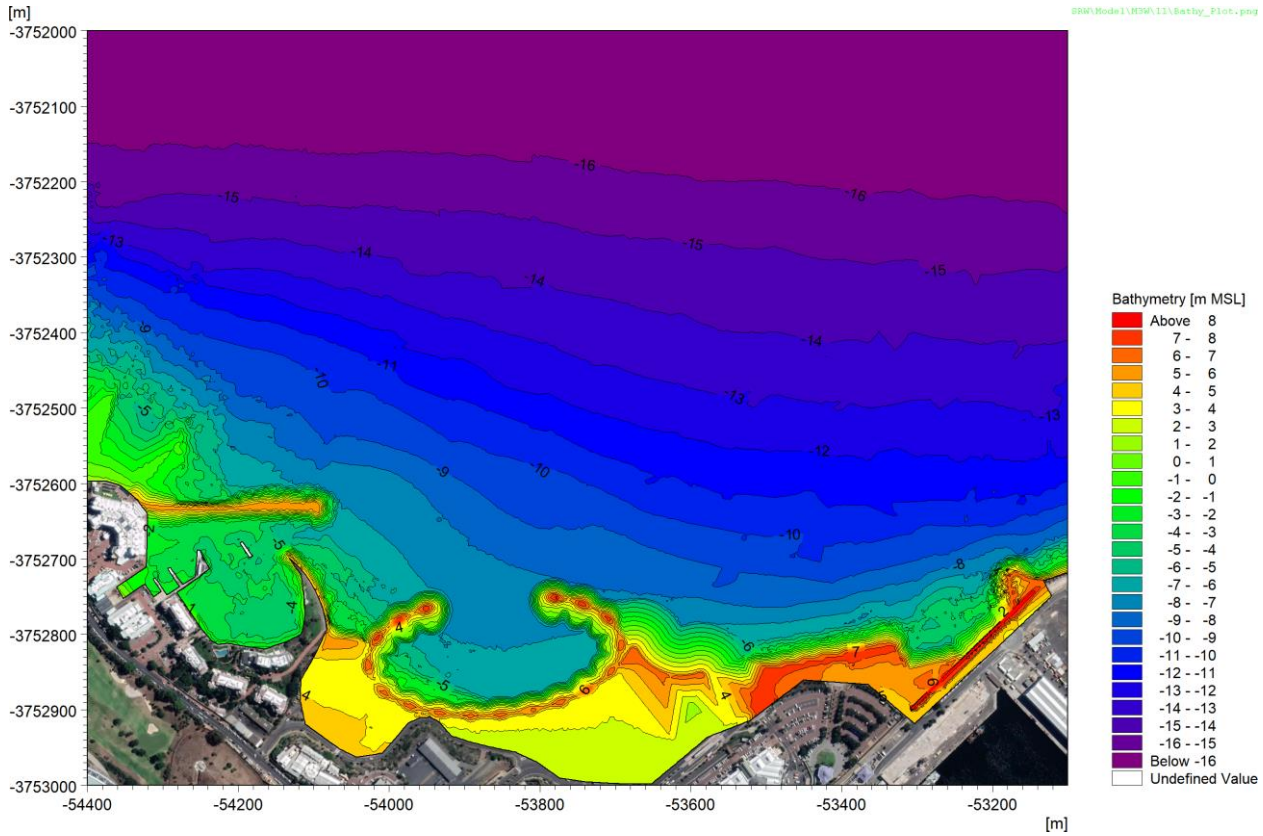

Figure 2-14: Detailed bathymetry for new development layout.

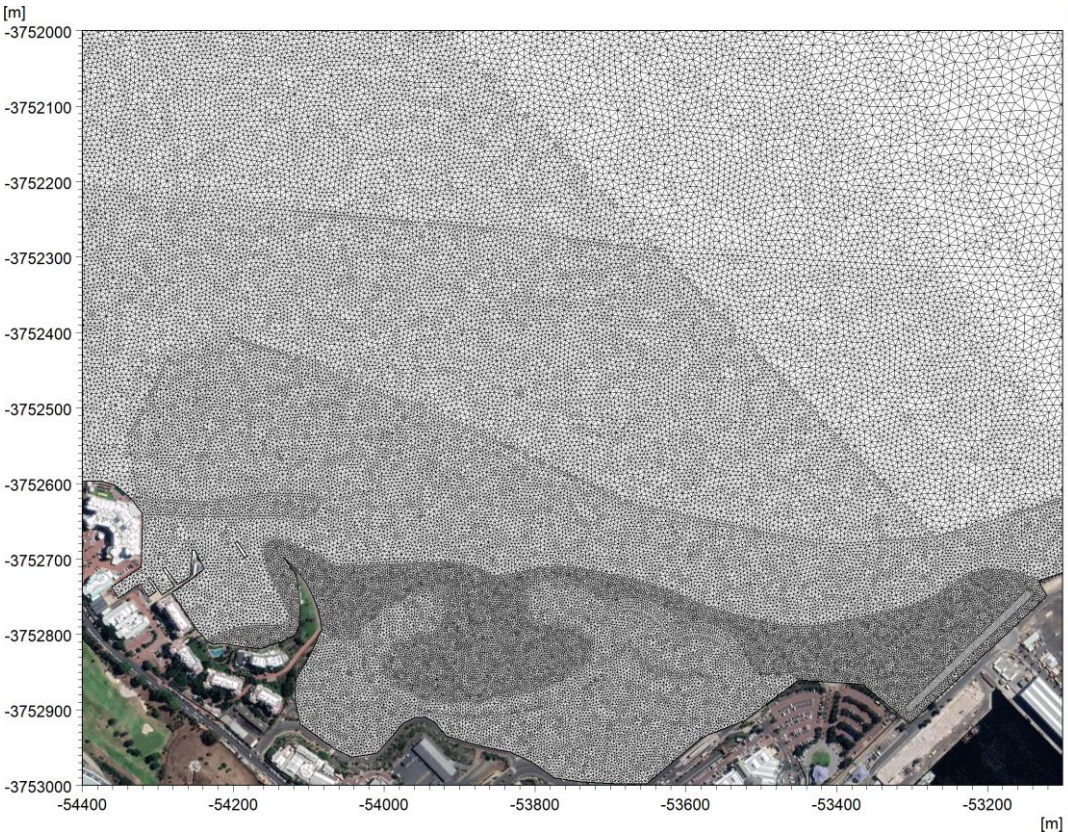

Figure 2-15: Detailed mesh for new development layout.

2.2.2.2 Model inputs

Bottom friction was modelled using the quadratic drag coefficient formulation. The friction coefficient was calibrated to each armouring and structure type in the model (rock slope, dolos slope and rock berm breakwater) by comparing to a detailed, porosity-based flume model. The porosity-based model can simulate the resistance of porous structures and more realistically reproduce wave reflection and run-up, however it is computationally intensive to do this at a full 3D scale. Therefore, flume models were used to obtain a calibrated friction value for each type of porous structure.

Each run consisted of 5 minutes of model spin-up and a further 60 minutes of the modelled sea state. The spin-up was ignored in all the results. Waves in the model were generated along the -20 m MSL contour on the north-western boundary.

2.2.3 Calibration

In the absence of measured water level or wave data in Granger Bay, a qualitative model calibration was undertaken by simulating a specific storm event and comparing the model results to photographs of wave run-up and overtopping taken at the corresponding date and time.

The storm of 13 July 2020 was used for the model calibration. A 1-hour sea state at 15:00 (UTC+2) was modelled using the offshore wave conditions at -20 m MSL obtained from the wave refraction model and measured water levels from Cape Town, as described in PRDW (2022). The model input conditions are presented in Table 2-2.

Table 2-2: Model inputs at 15:00 for the 13 July 2020 storm.

H_{m0} [m]	T_p [s]	MWD [deg]	DSD [deg]	Water Level [m MSL]
8.0	16.9	276	16	0.1

Figure 2-16 presents a snapshot of the instantaneous water surface elevations during the 13 July 2020 storm. This can be compared to Figure 2-17 and Figure 2-18 which show photographs of overtopping along the rock revetment and in front of the Grand Africa Café, respectively.

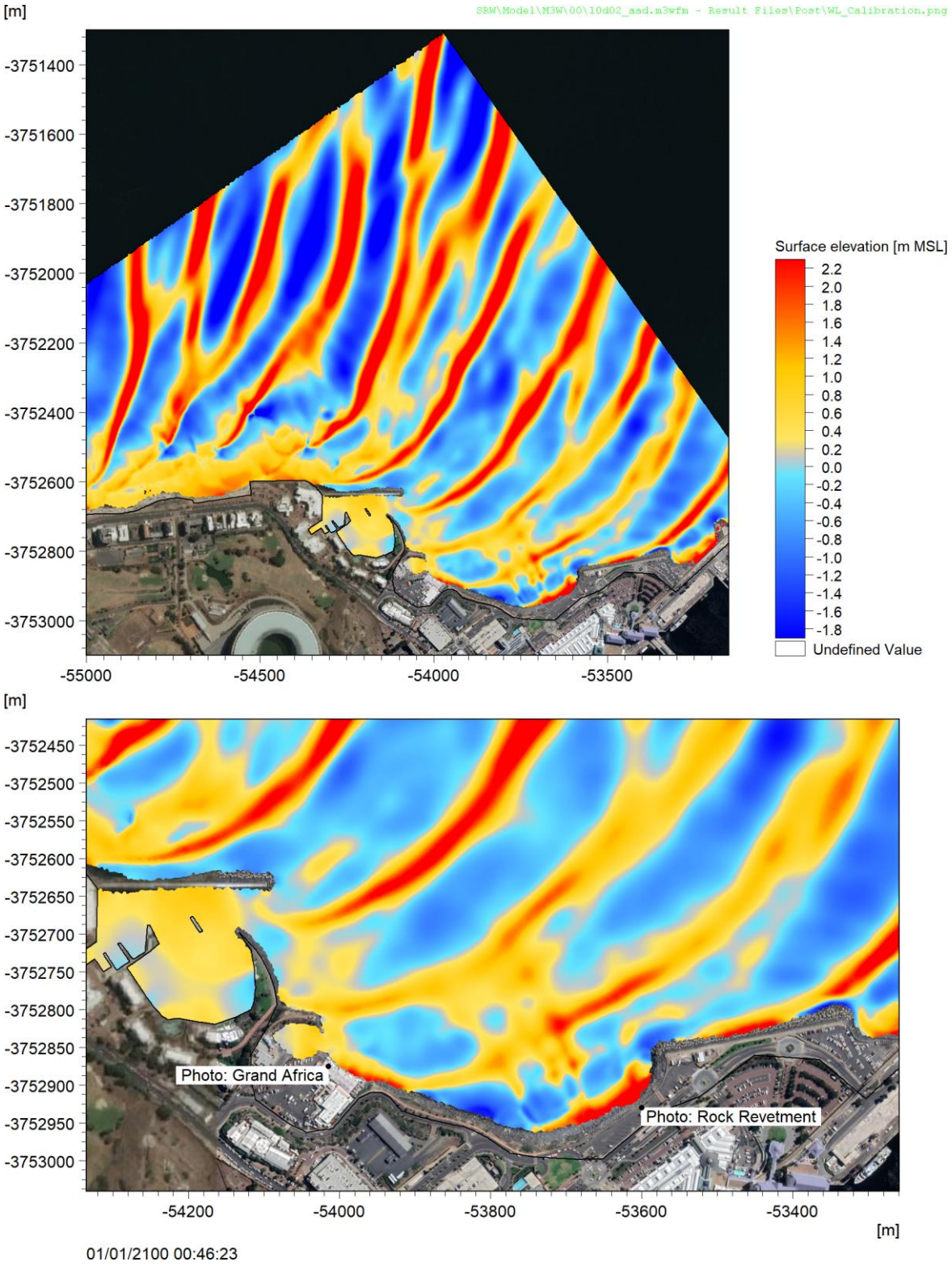

Figure 2-16: Instantaneous modelled surface elevation of an overtopping event during the 13 July 2020 storm.

Figure 2-17: Overtopping of rock revetment at approximately 15:00 on 13 July 2020. Photo credit: Stephen Luger.

Figure 2-18: Overtopping in front of Grand Africa Café on 13 July 2020 (exact time unknown). Photo credit: Anton Holtzhausen.

The snapshot presented in Figure 2-16 shows similar overtopping to the photos taken during the storm at both locations. Although this is not a quantitative comparison, this suggests that the model is accurately reproducing all the processes and as such can be considered to be sufficiently accurate for the purposes of this study.

2.2.4 Critical bed shear stress

Figure 2-19 shows the percentage of fines (sediment grain size <63 µm) obtained from a number of historical sediment sampling campaigns in Table Bay. The fines percentages in shallow areas exposed to waves are low. In deeper water offshore of Robben Island, the analyses shows fines percentages of approximately 10% to 15%. This suggests the temporary deposition of fine particulate matter, i.e. most of the time the bed shear

stresses are sufficiently low for deposition to occur, but resuspension occurs during storm events with large waves. The permanent depo-centres were identified by a percentage fines >20% and include the Koeberg intake basin, the Port of Cape Town and Murray's Harbour (on Robben Island).

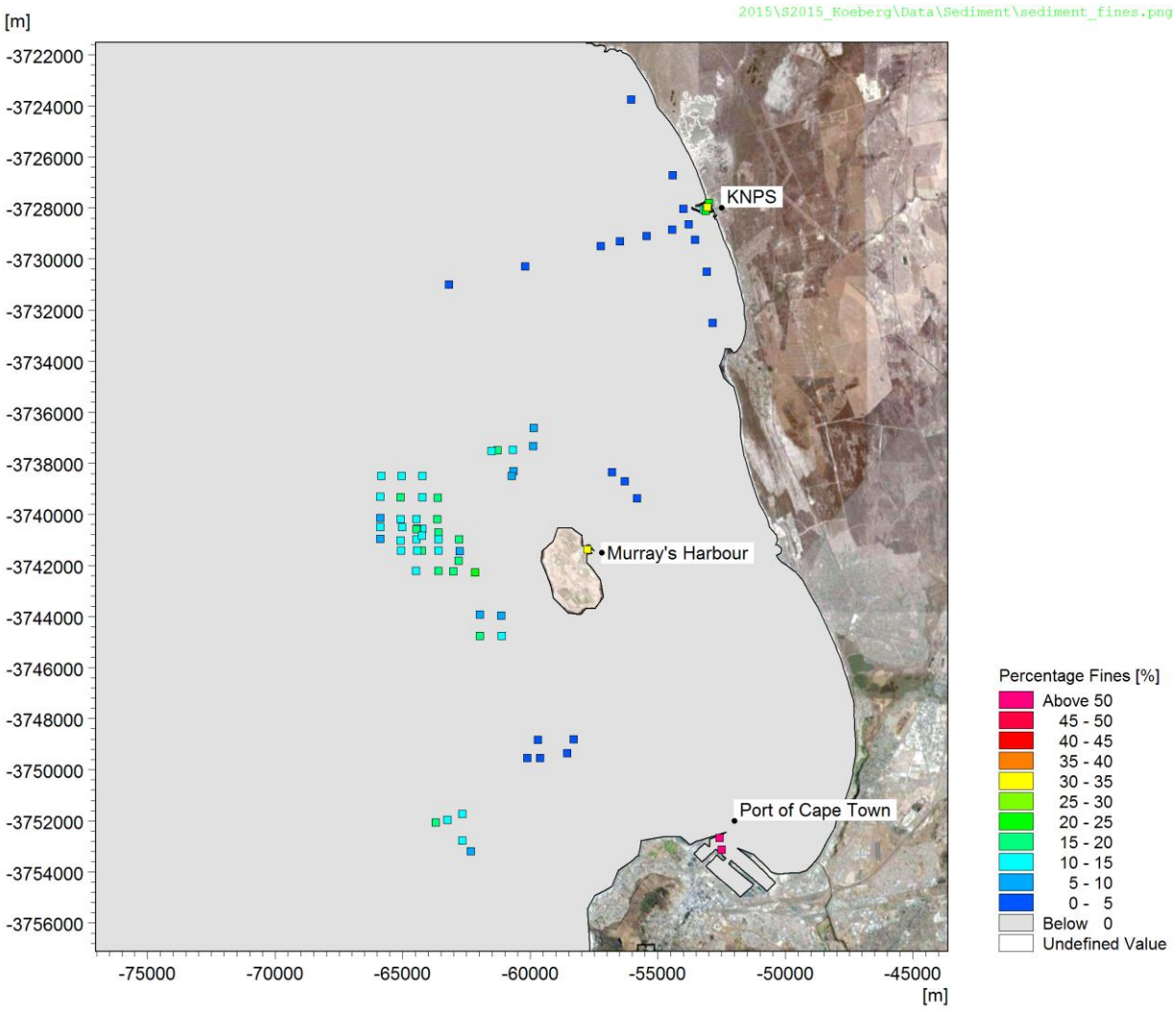

Figure 2-19: Percentage fines obtained from a number of historical sediment sampling campaigns.

Figure 2-20 shows the bed shear stresses modelled by PRDW at each location plotted against the measured percentage fines at the corresponding location. The expected behaviour is that areas with low bed shear stresses will have a higher fines percentage (muddy seabed), since the stresses during storm events are too low to resuspend the fines that are deposited during calm periods. As shown in the figure, this trend is supported. The distinction between permanent depo-centres (fines >20%, muddy) and areas with temporary or little deposition (fines <20%, sandy) is at a bed shear stress of approximately 0.2 N/m^2.

Based on these results, areas where the bed shear stress exceeds 0.2 N/m^2 during storm events will tend to be sandy, whilst areas where the bed shear stress remains below 0.2 N/m^2 will tend to be muddy.

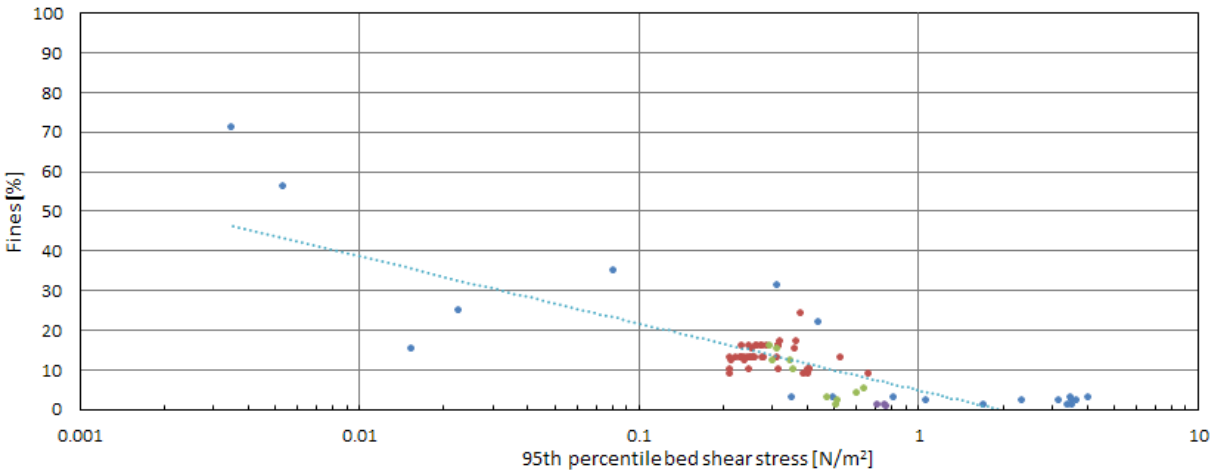

Figure 2-20: Correlation of the percentage fines measured in grab samples of the seabed sediment and the 95th percentile modelled bed shear stress.

In Granger Bay, the hydrodynamic model showed that the current speeds due to wind, tides and ocean currents are low and thus did not contribute significantly to the bed shear stresses, which are primarily driven by waves.

The phase-resolving wave model (as described in Sections 2.2.1 to 2.2.3) was used to calculate the wave-induced bed shear stresses using a bed roughness of 0.001 m and the wave-induced currents at the seabed time-averaged over the modelled sea-state duration of 45 minutes. These bed shear stresses include contributions from both swell waves (period <25 s) and longer period waves caused by bound waves, surf beat and harbour resonance.

Figure 2-21 shows the modelled wave-induced bed shear stresses in Granger Bay during a 1-year return period storm event. Areas where the bed shear stress exceeds 0.2 N/m^2 during storm events will tend to be sandy and are indicated in shades of blue, whilst areas where the bed shear stress remains below 0.2 N/m^2 will tend to be muddy and are indicated in shaded of brown. The modelled wave-induced bed shear stresses were compared to the high-resolution bathymetric surveys of the Waterclub and Granger Bay shown in Figure 2-23 and Figure 2-22.

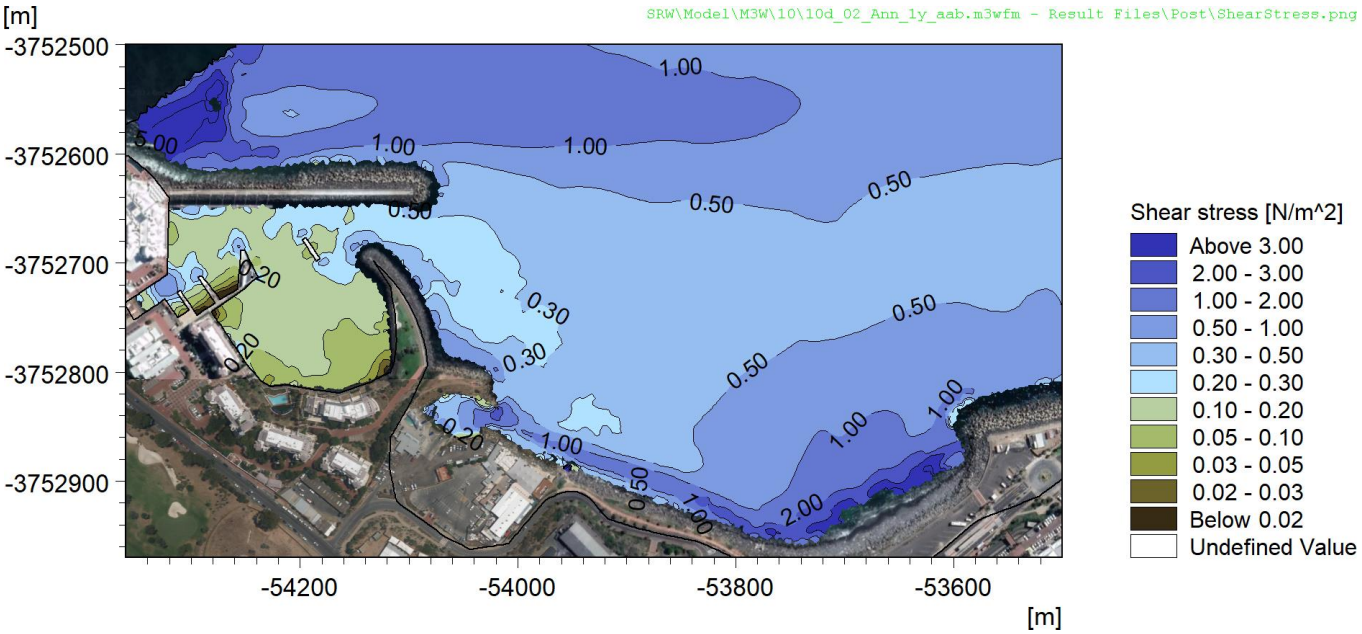

Figure 2-21: Modelled bed shear stresses during 1-year return period storm.

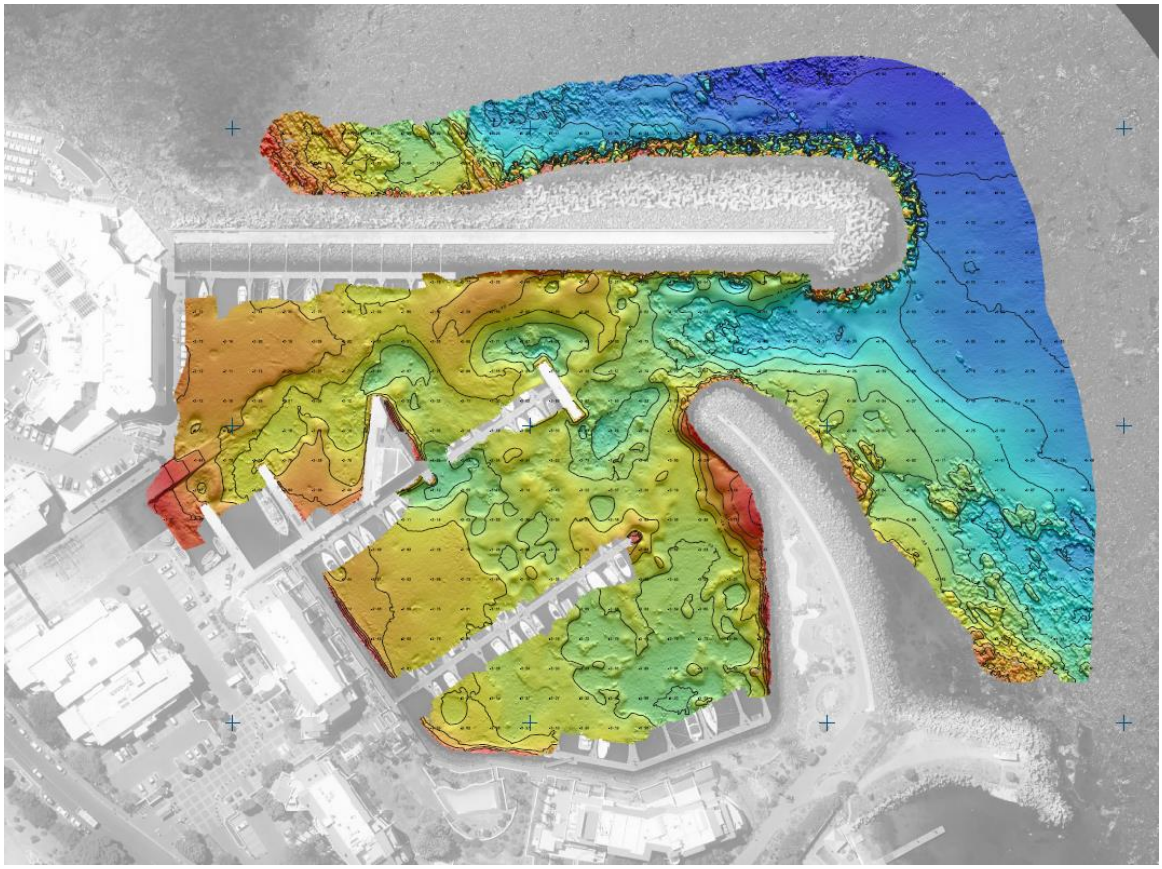

Figure 2-22: High-resolution bathymetric survey of the Waterclub (Tritan Survey, 2021)

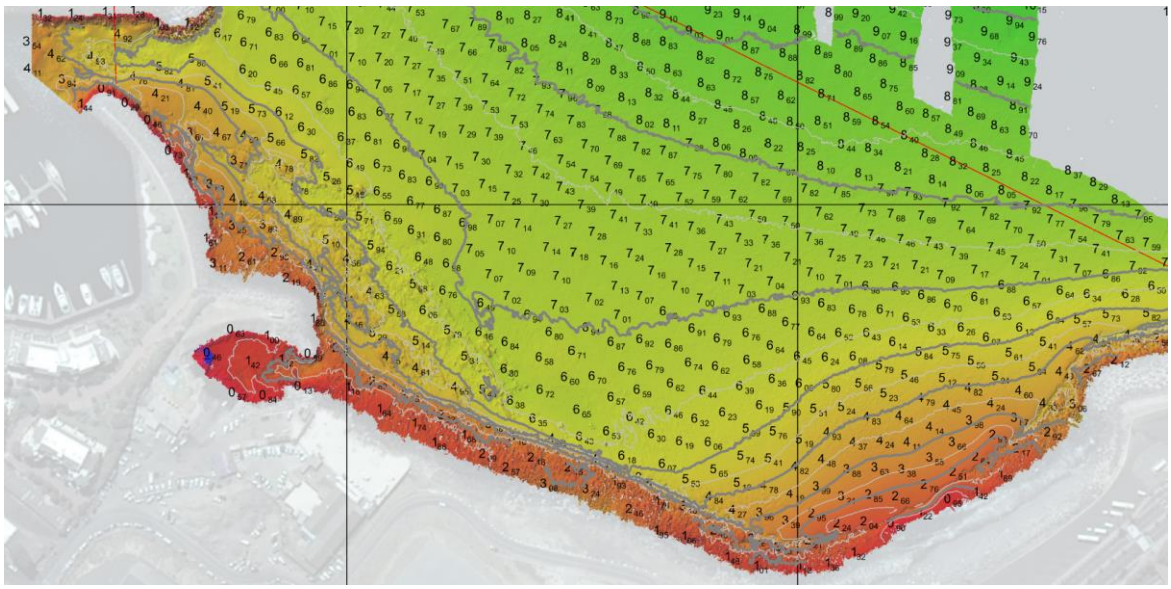

Figure 2-23: High-resolution bathymetric survey of Granger Bay (Underwater Surveys, 2022).

The Waterclub survey indicates a muddy seabed inside the marina, except at the entrance and adjacent to the non-floating quay wall west of the entrance where there are scour holes induced by strong currents due to harbour resonance. This is consistent with the model results which predict mud inside the marina except at the scour holes mentioned above.

The Granger Bay survey shows rocky areas along the shoreline north and east of Oceana, with what appears to be a sandy bottom over the remainder of the bay. This is consistent with the model results which predict sand everywhere except inside the Waterclub.

This comparison suggests that the model well represents the wave-induced bed shear stresses around the site and confirms that the use of 0.2 N/m^2 as the critical shear stress for long-term mud accumulation.

2.2.5 Cases modelled

The wave model needed to be representative of the storm wave climate over the year. Fines are expected to be deposited during all calm periods. To check whether these fines will accumulate for long periods or will be resuspended during storms, the average 1-month return period storm during summer, the average 1-month return period storm during winter as well as the average 1-year return period storm were modelled.

The 1-year return period was determined from the extreme value analysis (EVA) described in PRDW (2022). The 1-month return periods for summer and winter were determined from a year of modelled waves. A typical year of waves was simulated at the wave model boundary at a depth of -20 m MSL using the same spectral wave model described in PRDW (2022). A time series of these waves is presented in Figure 2-24 with the 1-month summer, 1-month winter and 1-year significant storm wave heights (H_{m0}) indicated.

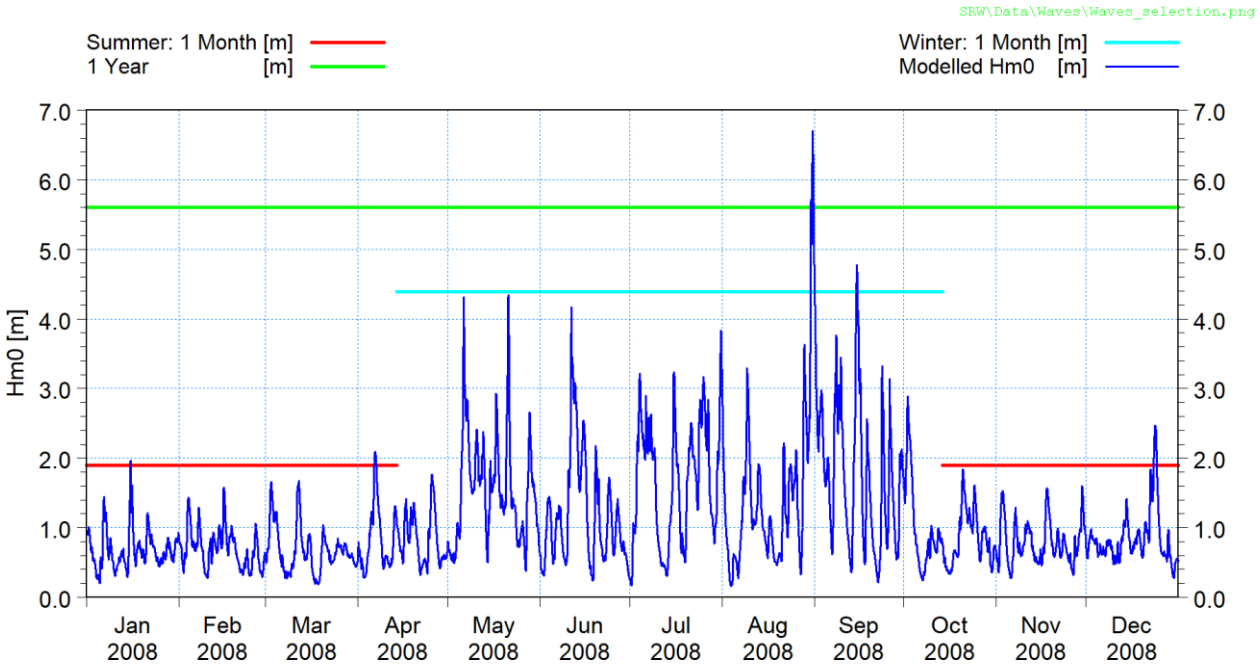

Figure 2-24: Time series of H_{m0} at -20 m MSL for a representative year with 1-month summer, 1-month winter and 1-year return period significant storm wave heights indicated.

After selecting the H_{m0}, typical peak wave periods (T_p), mean direction at T_p (D_{mTp}) and directional standard deviations (DSD) were assigned to each condition based on the data from the modelled year. The wave conditions are presented in Table 2-3 below.

Table 2-3: Wave parameters in -20 m MSL.

Season	Return Period	H_{m0} [m]	T_p [s]	D_{mTp} [deg]	DSD [deg]
Summer	1 month	1.9	13	268	16
Winter	1 month	4.4	14	280	16
Annual	1 year	5.6	14	280	16

3. RESULTS

3.1 Current speed and direction

This section presents the results of the current speed due to wind, tides and ocean currents only, excluding wave-driven currents which are included in the wave-induced bed shear stresses described in Section 3.4.

Instantaneous depth-averaged current speeds and vectors during a south-easterly wind event are presented in Figure 3-1, while Figure 3-2 presents the instantaneous current speeds and vectors during a north-westerly event. The maximum (99th percentile) current speeds during the 6-week simulation for summer/autumn are presented in Figure 3-3 and for winter/spring in Figure 3-4. As the current speeds around the study site are very low, only the maximum currents (defined for robustness as the 99th percentile current speed over the 6-week simulation) are presented.

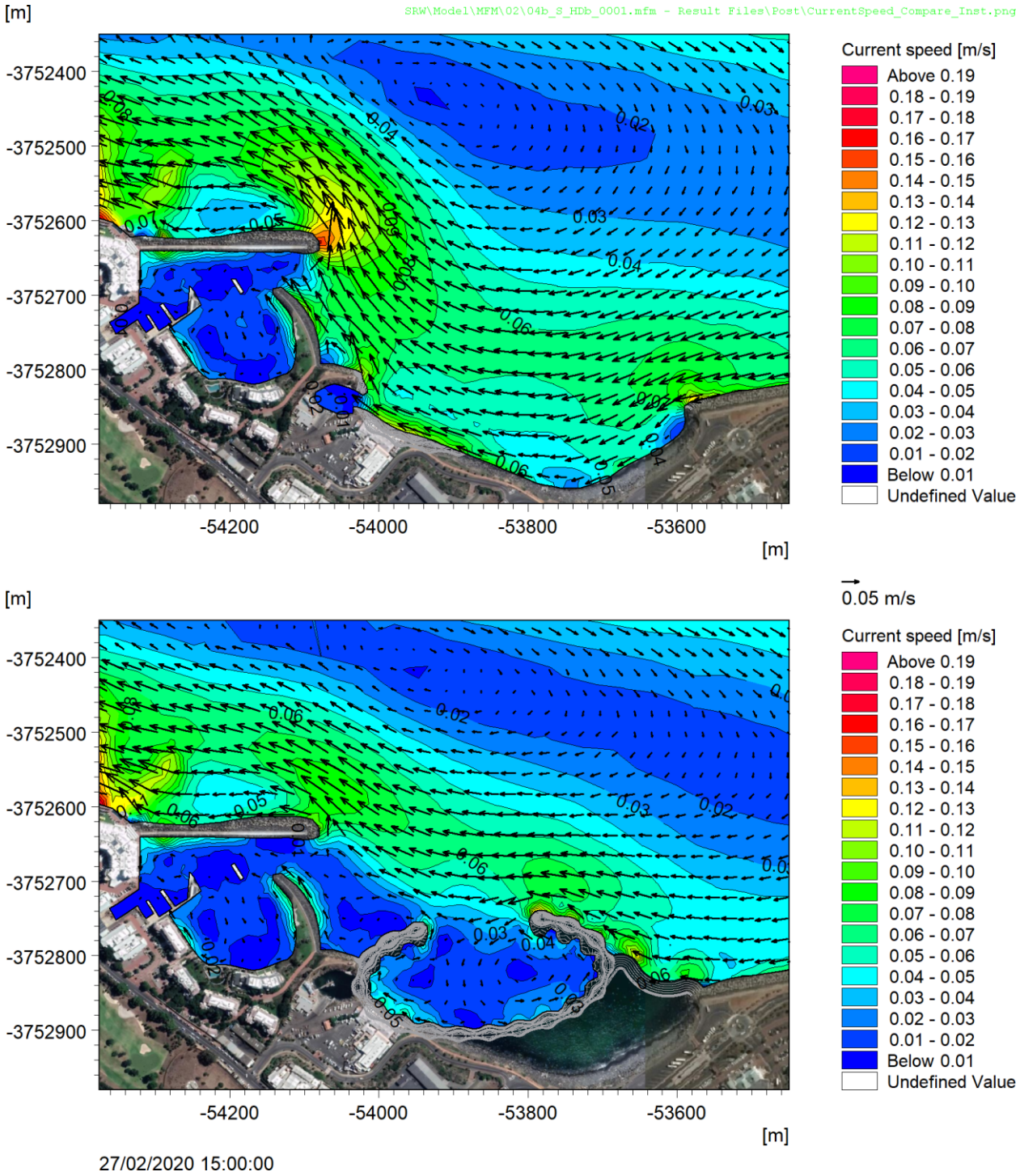

Figure 3-1: Instantaneous depth-averaged current speed during a south-easterly wind event for the baseline (top) and development (bottom) layouts.

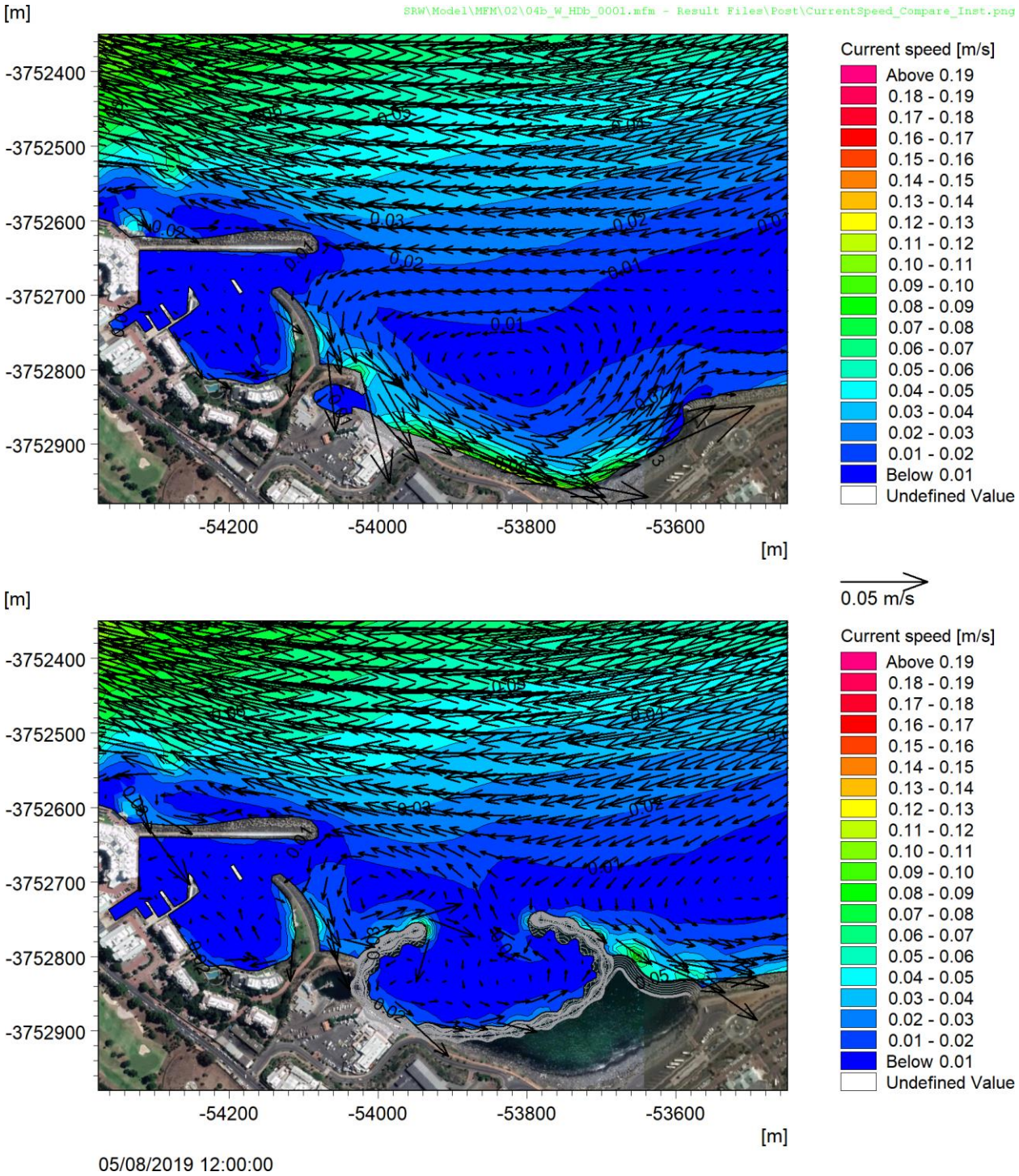

Figure 3-2: Instantaneous depth-averaged current speed during a north-westerly wind event for the baseline (top) and development (bottom) layouts.

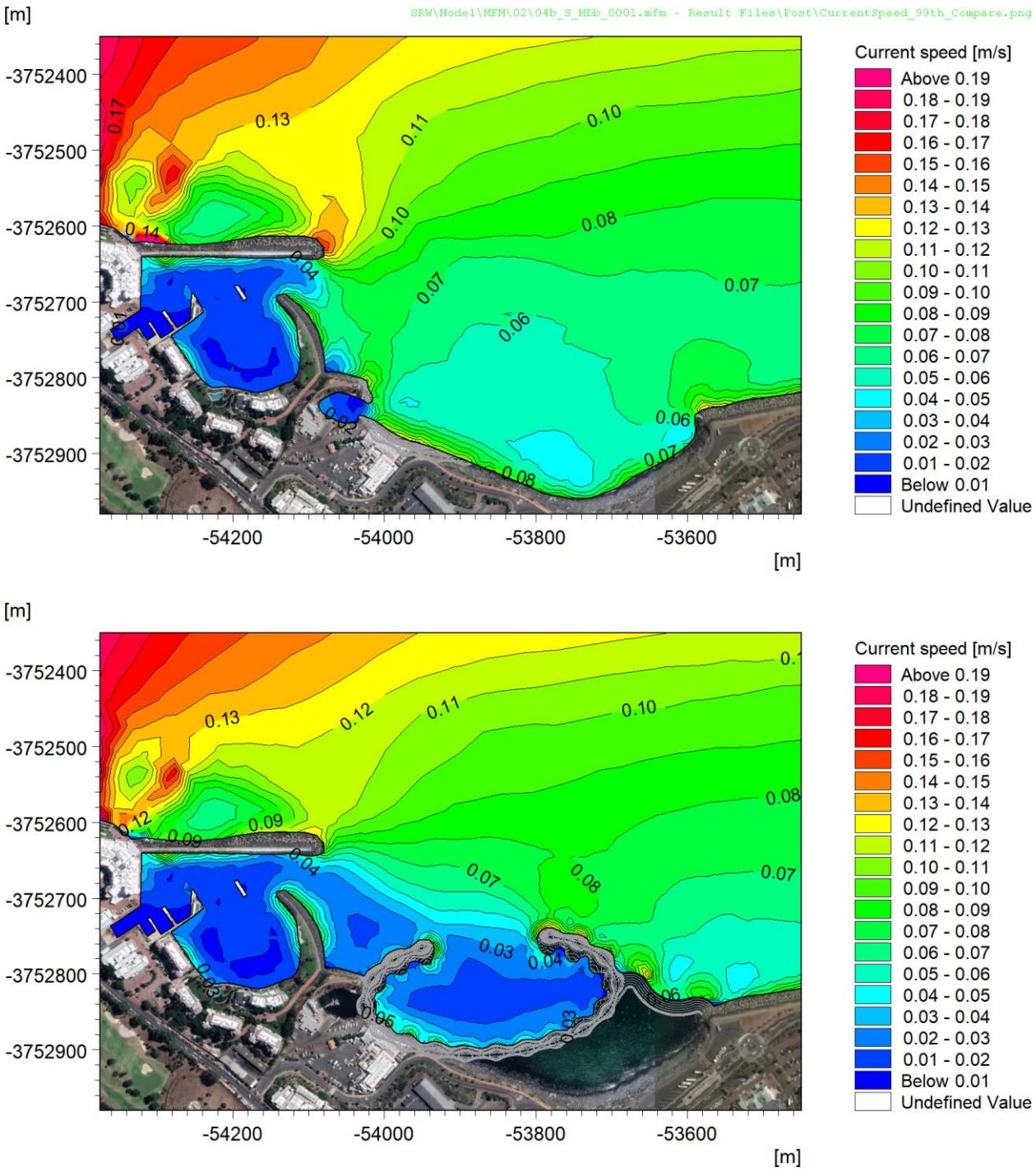

Figure 3-3: Maximum (99th percentile) depth-averaged current speed for the baseline (top) and development (bottom) layouts for the summer/autumn case.

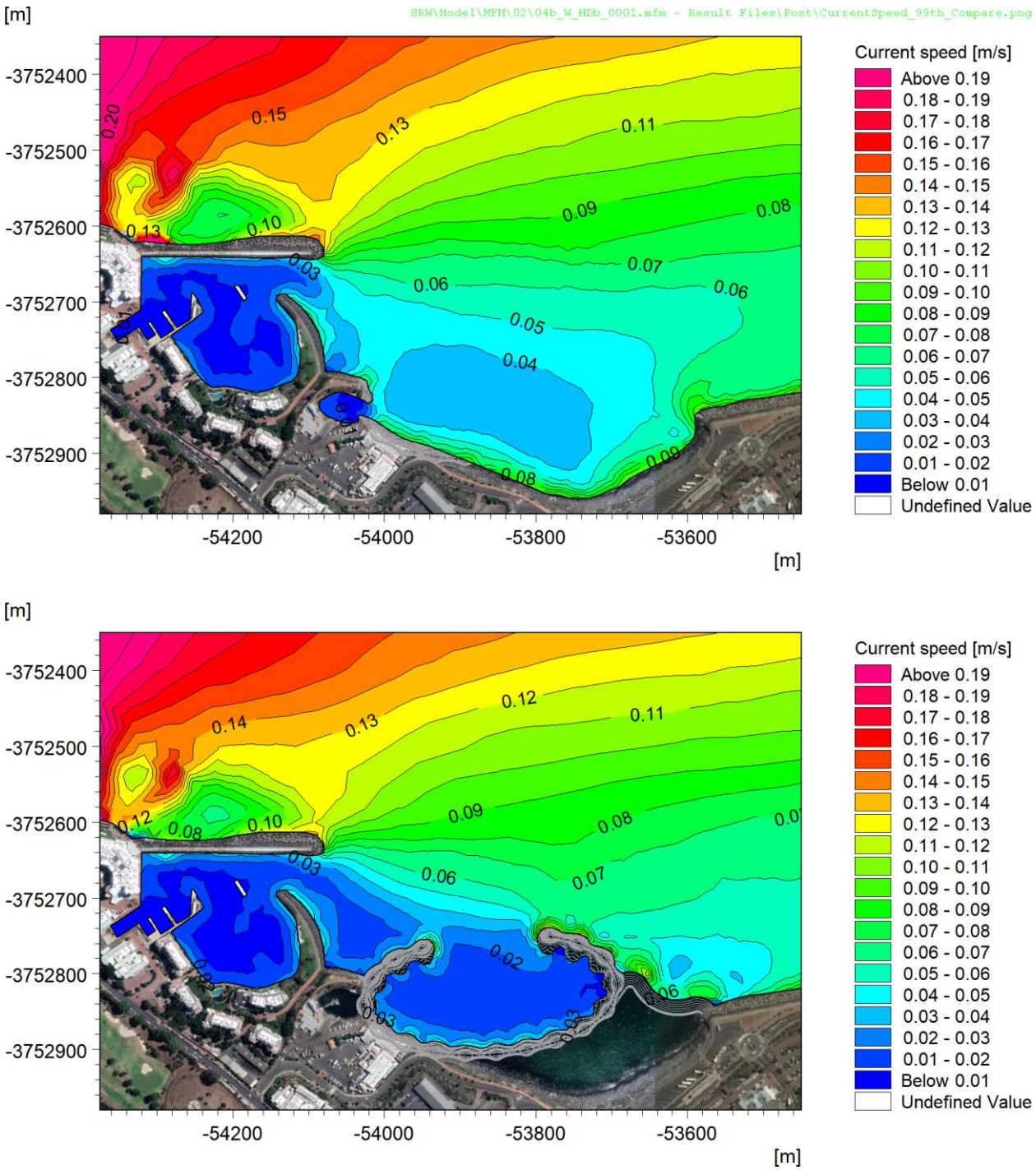

Figure 3-4: Maximum (99th percentile) depth-averaged current speed for the baseline (top) and development (bottom) layouts for the winter/spring case.

The model results inside the development layout are compared to the baseline layout. In addition, the results inside the development layout are compared to those inside the existing Waterclub marina, since this may assist with the marine ecological assessment.

The figures above show that:

- The current speeds in Granger Bay due to wind, tides, and ocean currents are very low with speeds generally not exceeding 0.1 m/s.

- The addition of the development reduces the maximum current speed inside the development from 0.06 m/s in summer and 0.04 m/s in winter to 0.02 m/s.
- The maximum current speeds inside the new development are higher (0.02 m/s) than those inside the Waterclub (0.01 m/s).
- The development does not change the currents significantly beyond 300 m from the development.

3.2 Flushing of water and seawater temperature

The depth-averaged residual current was calculated to provide an estimate of circulation patterns with and without the development. These residual currents are calculated as the vector average of the depth-averaged velocities over the 6-week simulation for summer/autumn and winter/spring and are presented in Figure 3-5 and Figure 3-6, respectively.

The maximum (99^{th} percentile) surface seawater temperature is presented to show the effect of the new development for summer/autumn and winter/spring in Figure 3-7 and Figure 3-8. Note that these are only the maximum temperatures during the 6-week simulation periods and not an estimate of the absolute maximum temperatures that can be expected. They do however provide a robust estimate of the increase in temperature inside the development.

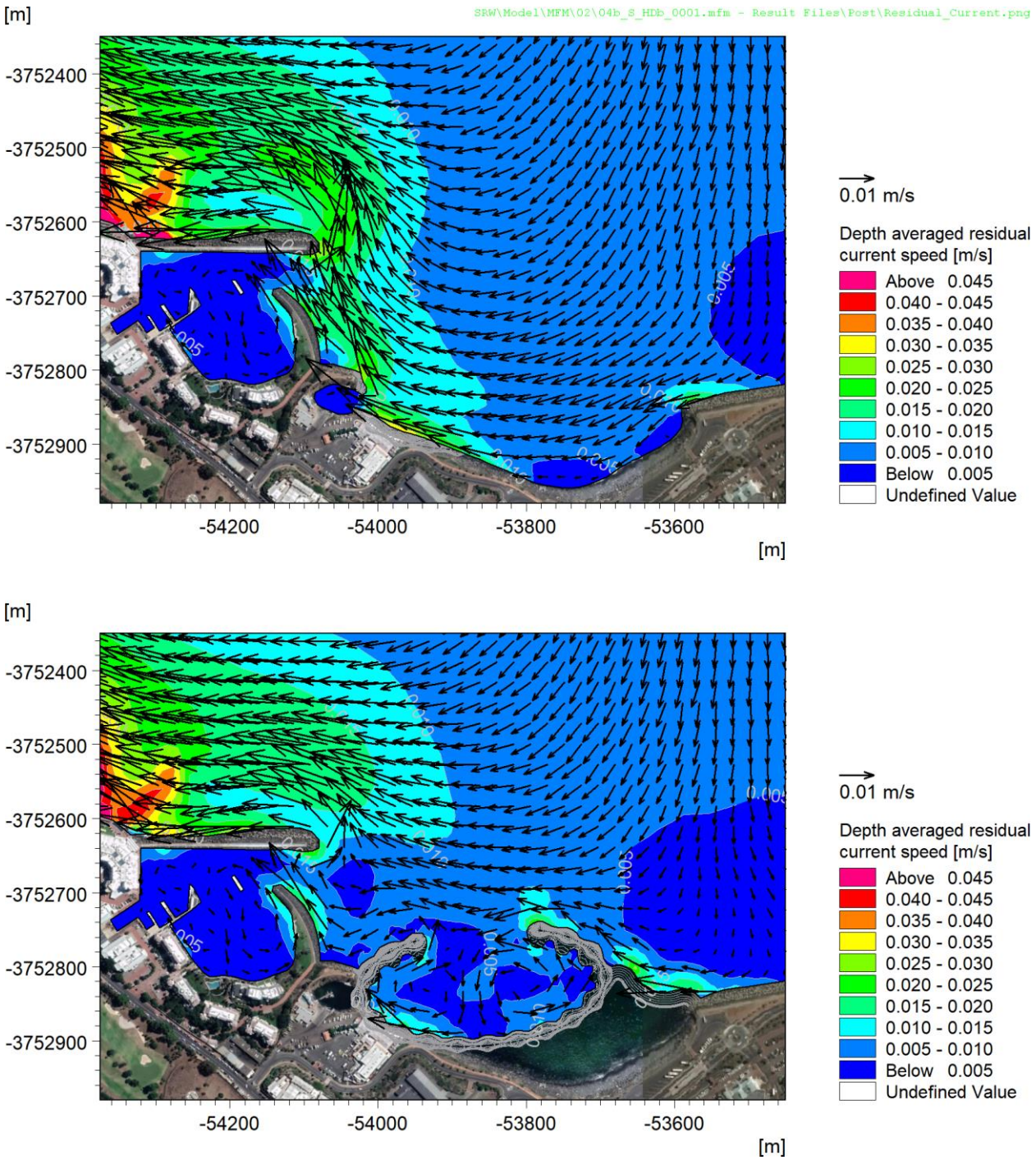

Figure 3-5: Depth-averaged residual currents for the baseline (top) and development (bottom) layouts for the summer/autumn case.

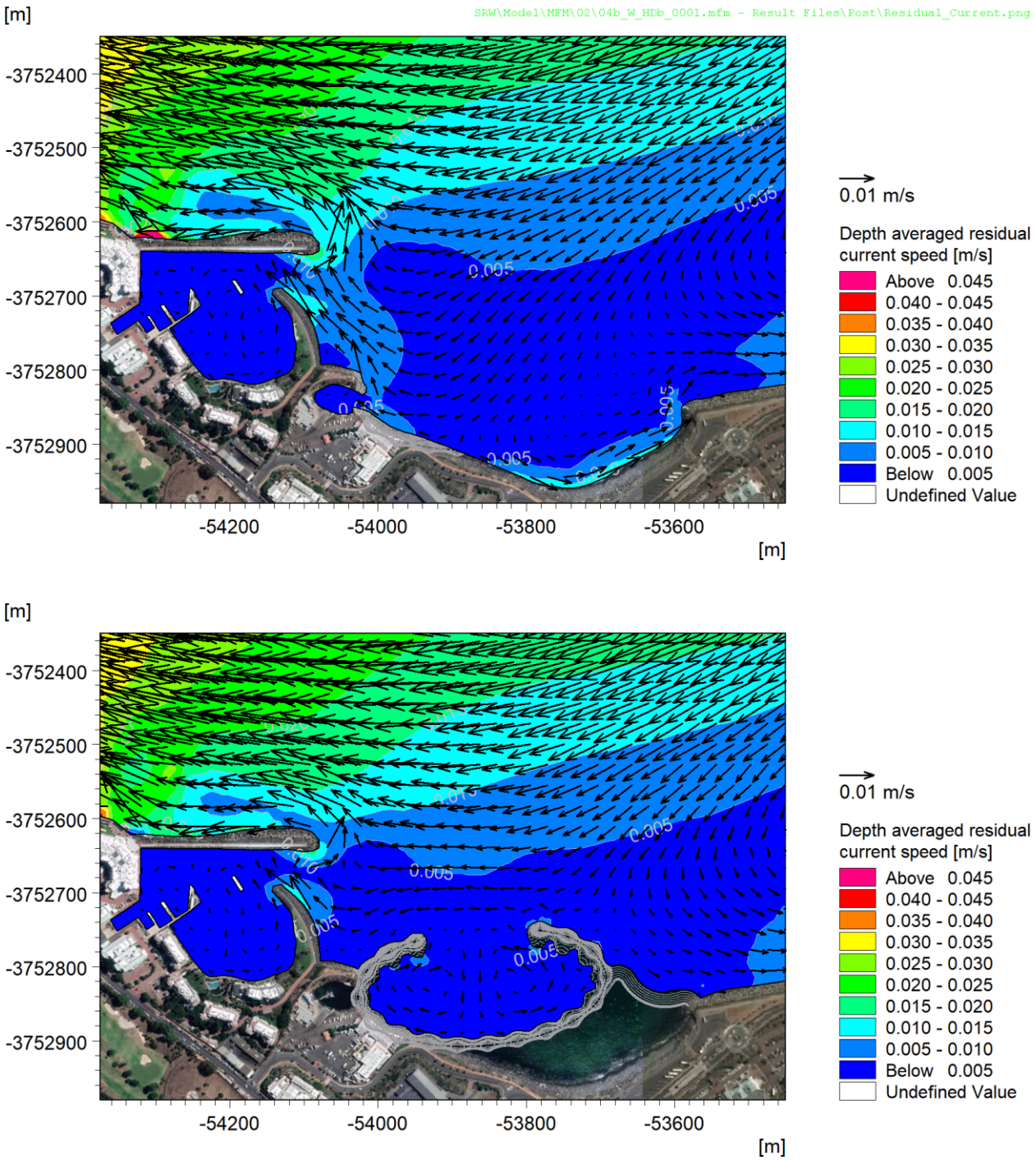

Figure 3-6: Depth-averaged residual currents for the baseline (top) and development (bottom) layouts for the winter/spring case.

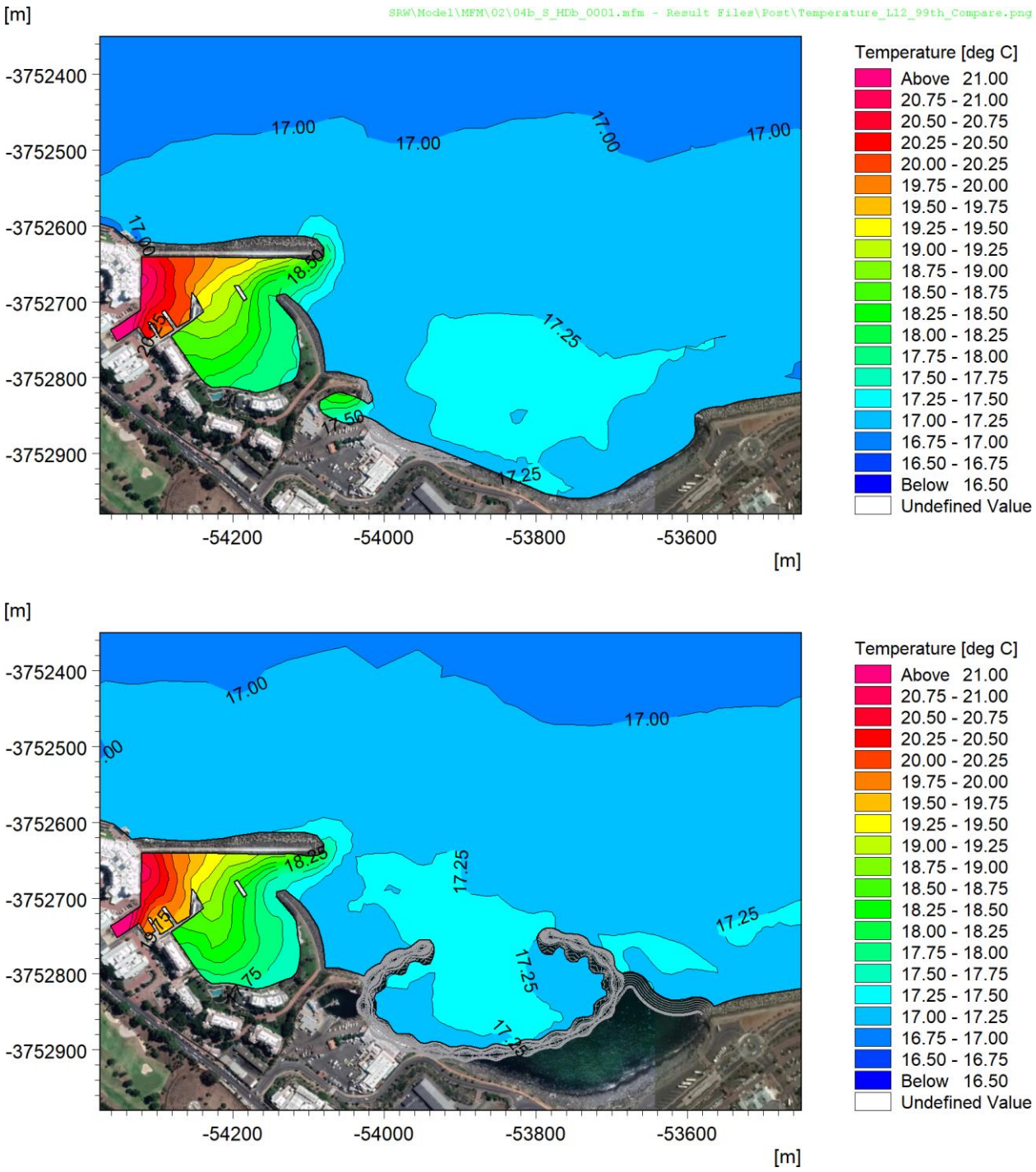

Figure 3-7: Maximum (99th percentile) surface seawater temperature for the baseline (top) and development (bottom) layouts for the summer/autumn case.

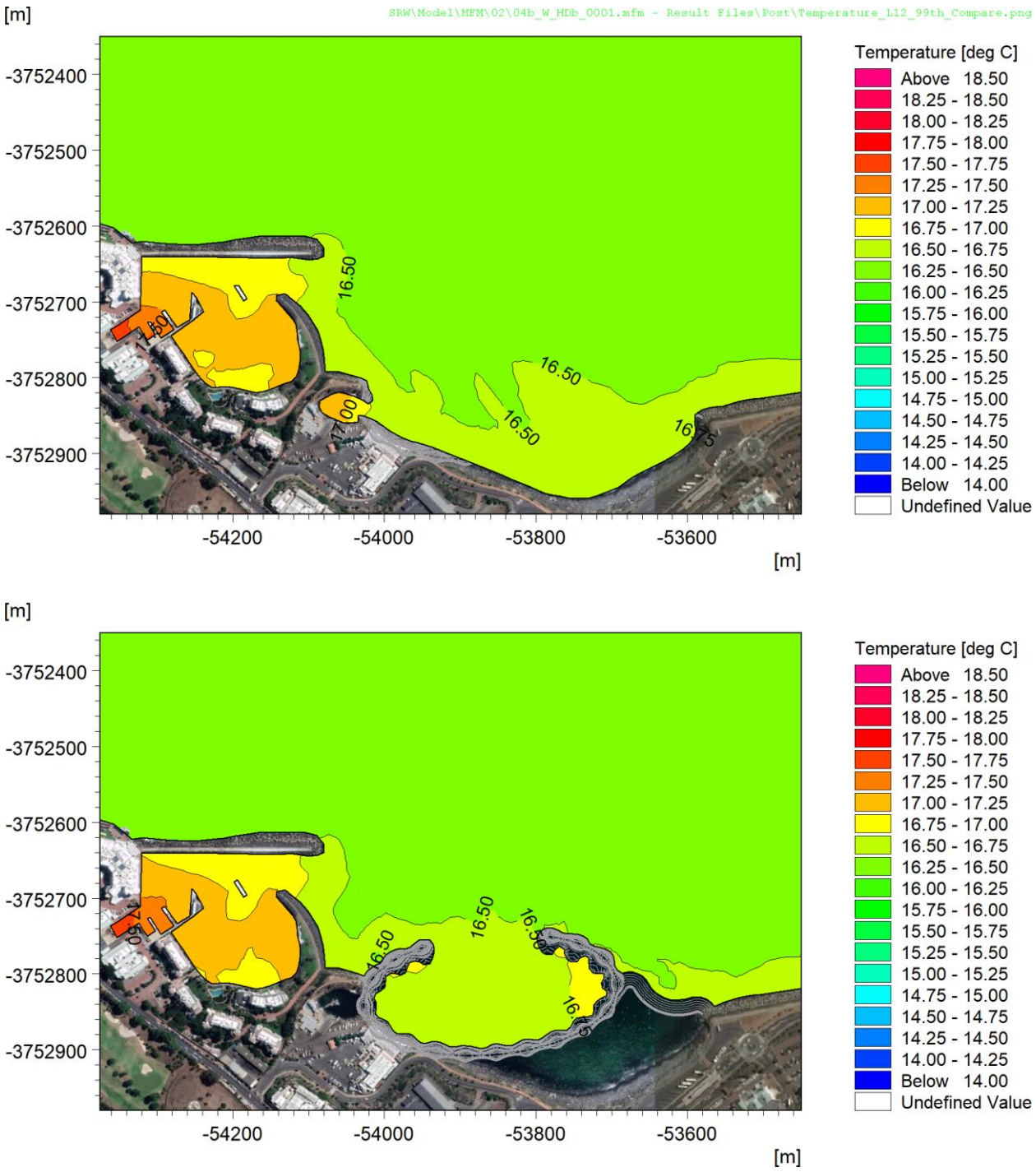

Figure 3-8: Maximum (99th percentile) surface seawater temperature for the baseline (top) and development (bottom) layouts for the winter/spring case.

The figures above show that:

- The residual circulation inside the new development comprises twin eddies which will induce flushing of water out of the development.
- The residual circulation is stronger in summer/autumn due to the strong south-east winds.
- The residual circulation within the development is slightly weaker than the baseline circulation, but stronger than the circulation within the Waterclub.

- The maximum surface seawater temperature inside the development area increases slightly (by about 0.25°C) in the winter/spring case, but remains the same in summer/autumn. This is explained by the stronger residual circulation in summer/autumn which does not allow a temperature build-up despite a net input of solar radiation in summer.
- The weaker residual circulation within the Waterclub results in a build-up in seawater temperature inside the Waterclub marina, particularly in summer.

3.3 Wave heights

The total significant wave heights (H_{m0}) for each wave condition are presented in this section for the baseline and development layouts. These total wave heights include both swell waves (period <25 s) and longer period waves caused by bound waves, surf beat and harbour resonance. The following three wave cases were modelled: 1-month return period storm in summer, 1-month return period storm in winter and 1-year return period storm.

Figure 3-9 presents an example of the instantaneous water surface elevations for the 1-year return period storm, which shows the individual wave crests (warm colours) and troughs (cool colours) as well as the processes of wave refraction, diffraction, reflection and harbour resonance. The H_{m0} results are shown in Figure 3-10 to Figure 3-12.

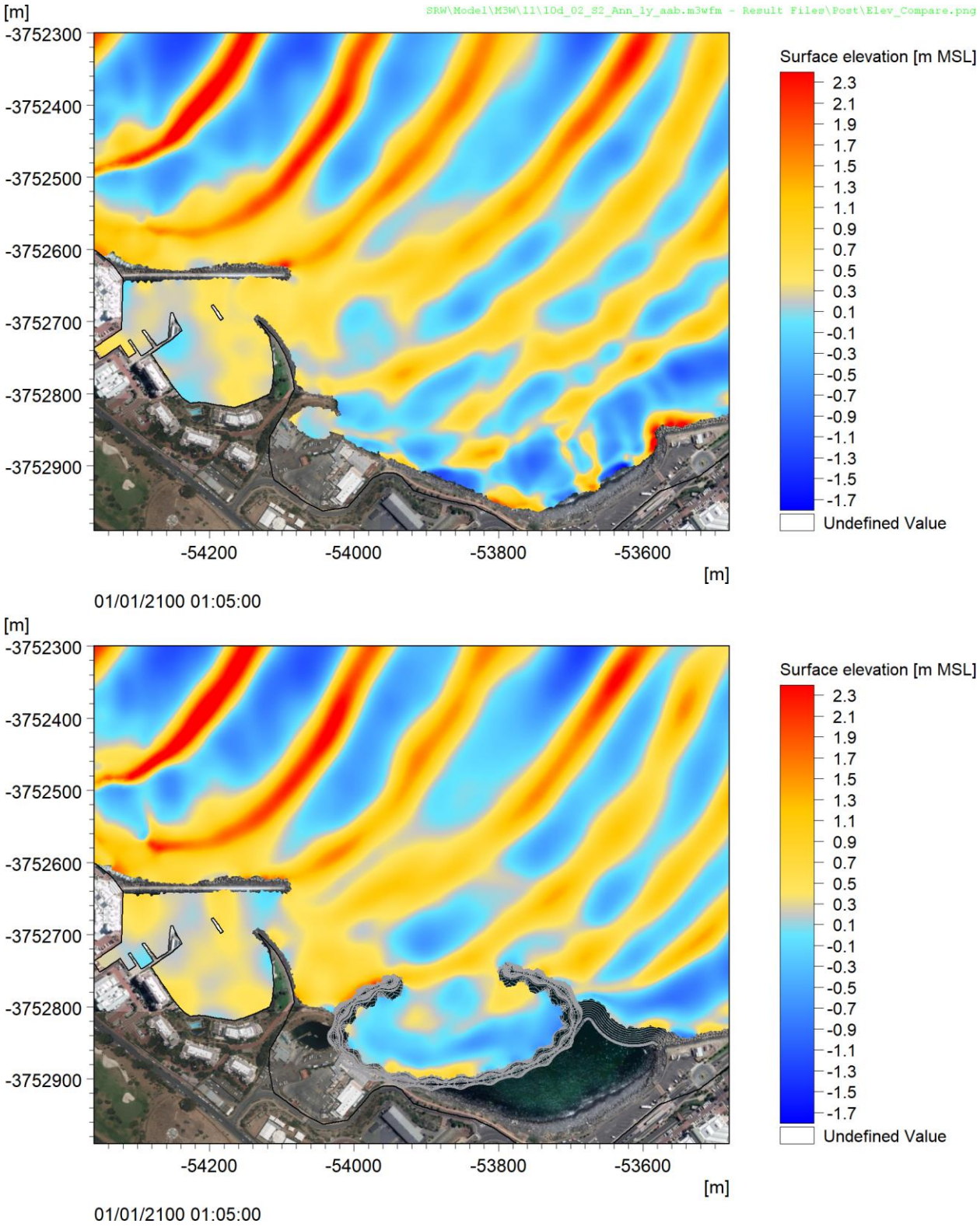

Figure 3-9: instantaneous water surface elevations for baseline (top) and development (bottom) layouts for the 1-year return period.

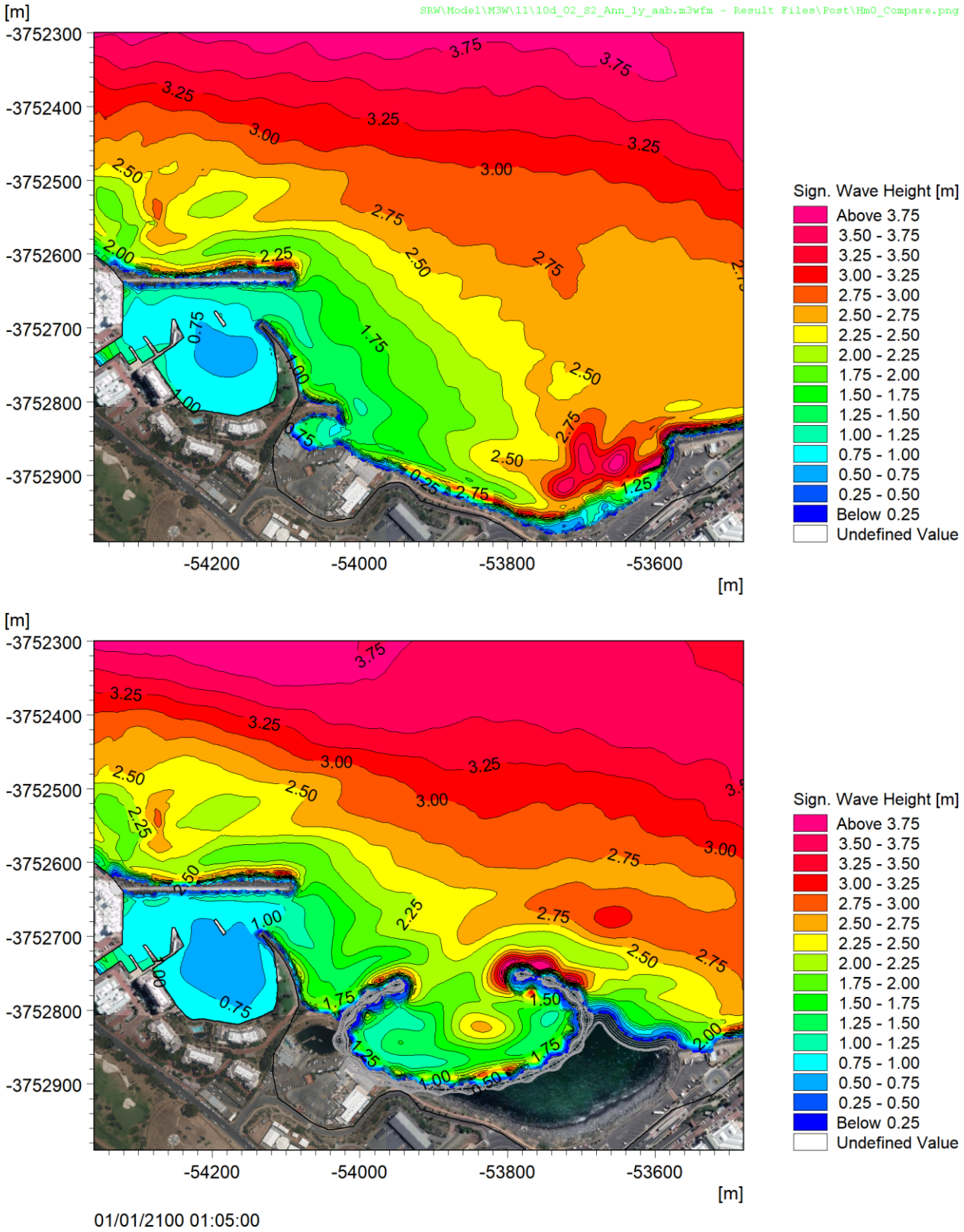

Figure 3-10: Total H_{m0} for baseline (top) and development (bottom) layouts for the 1-year return period.

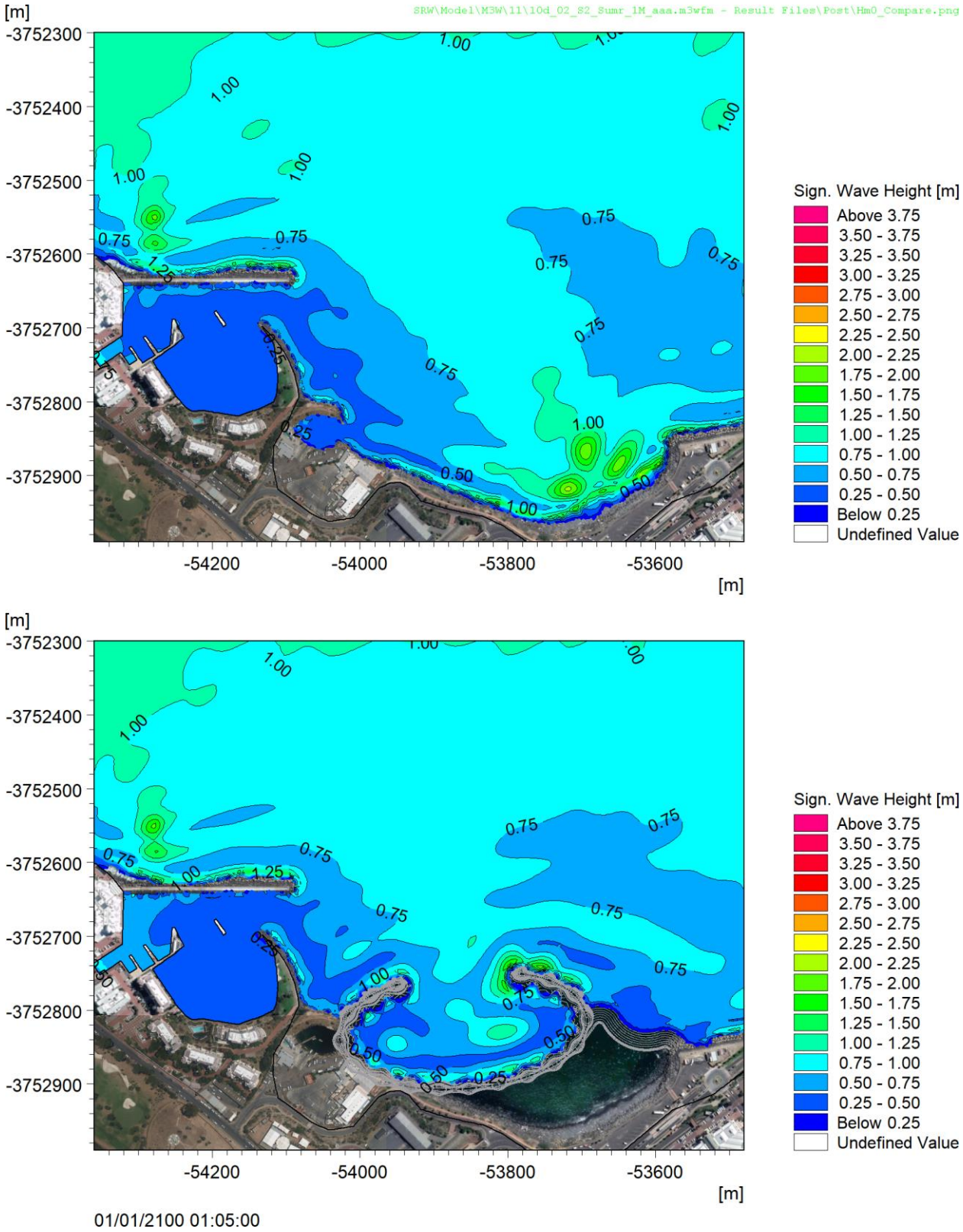

Figure 3-11: Total H_{m0} for baseline (top) and development (bottom) layouts for the 1-month return period in summer.

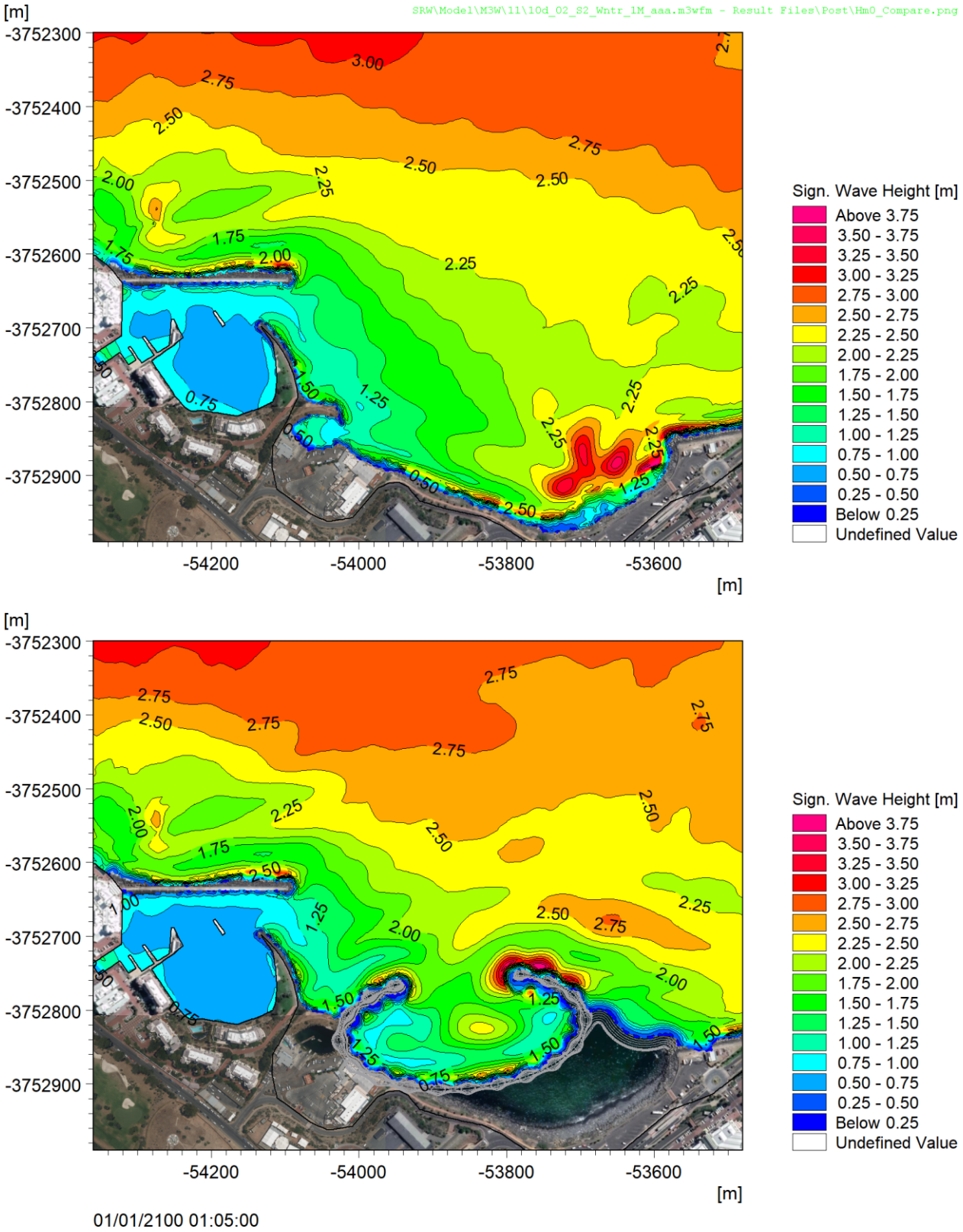

Figure 3-12: Total H_{m0} for baseline (top) and development (bottom) layouts for the 1-month return period in winter.

The figures above show that:

- The wave height inside the development is generally reduced compared to the baseline layout, however there is significant amplification in the centre of the development due to harbour resonance.

- The wave height inside the development is significantly larger than those inside the Waterclub.
- The wave height inside the Waterclub is slightly reduced by the development.
- The reflections off the eastern breakwater of the development generate nodes and anti-nodes, changing the wave height to the north-east of the development by up to 0.5 m for up to 300 m away from the structure. However, the development does not change the wave heights significantly beyond 500 m from the development.

3.4 Accumulation of mud

The existing seabed in Granger Bay is generally sandy because during large wave events any mud that is deposited during calm periods is resuspended, but it is possible that the new development will reduce the waves sufficiently to reduce the resuspension of mud and thus increase the percentage of mud on the seabed, with associated changes in marine ecology.

As described in Section 2.2.4, the wave model results have been processed to obtain the wave-induced bed shear stresses. The results for the three wave storm cases considered are presented in Figure 3-13 to Figure 3-15. Areas where the bed shear stress exceeds 0.2 N/m^2 during storm events will tend to be sandy and are indicated in shades of blue, whilst areas where the bed shear stress remains below 0.2 N/m^2 will tend to be muddy and are indicated in shaded of brown.

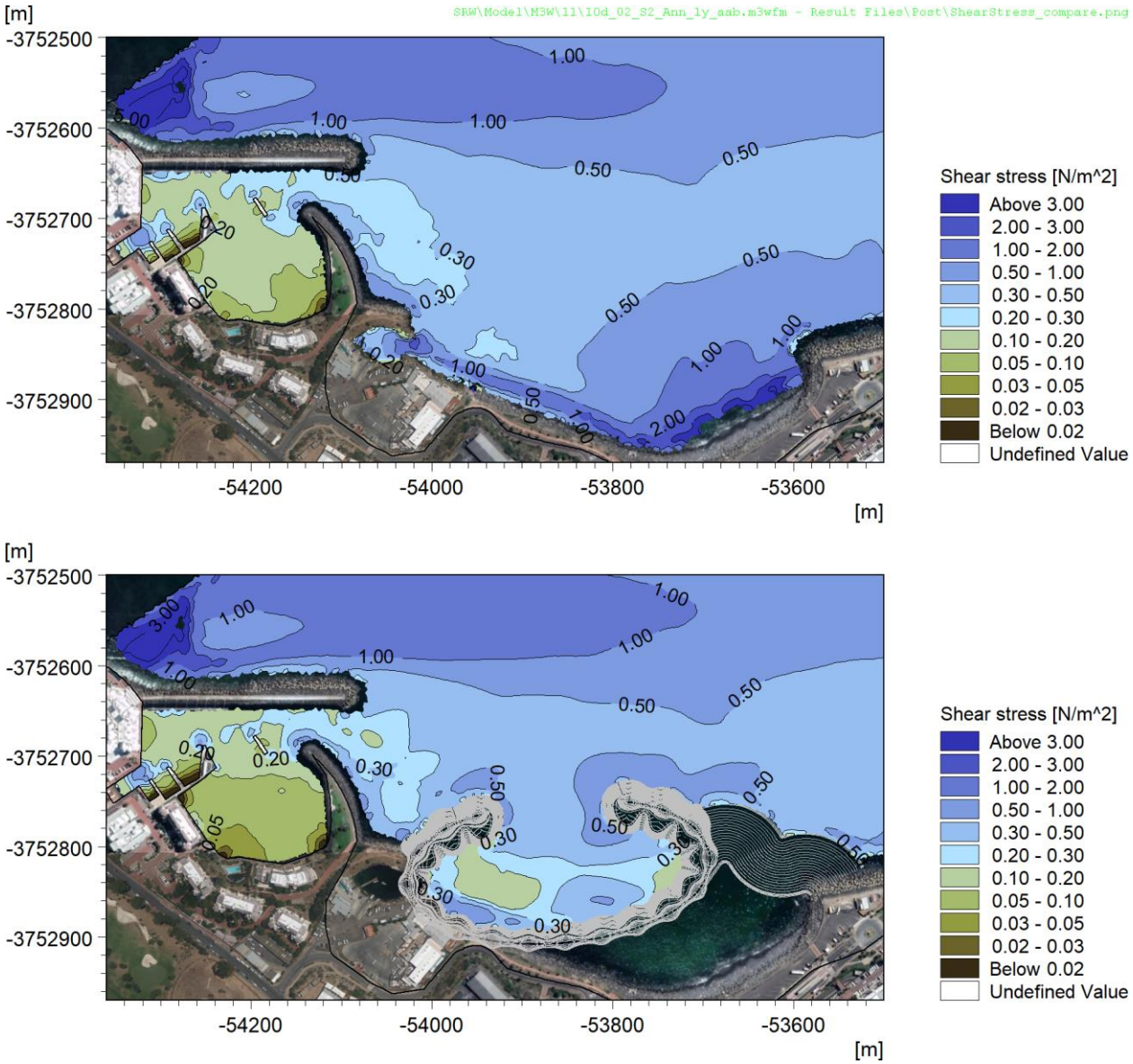

Figure 3-13: Wave-induced bed shear stress for baseline (top) and development (bottom) layouts for the 1-year return period storm event.

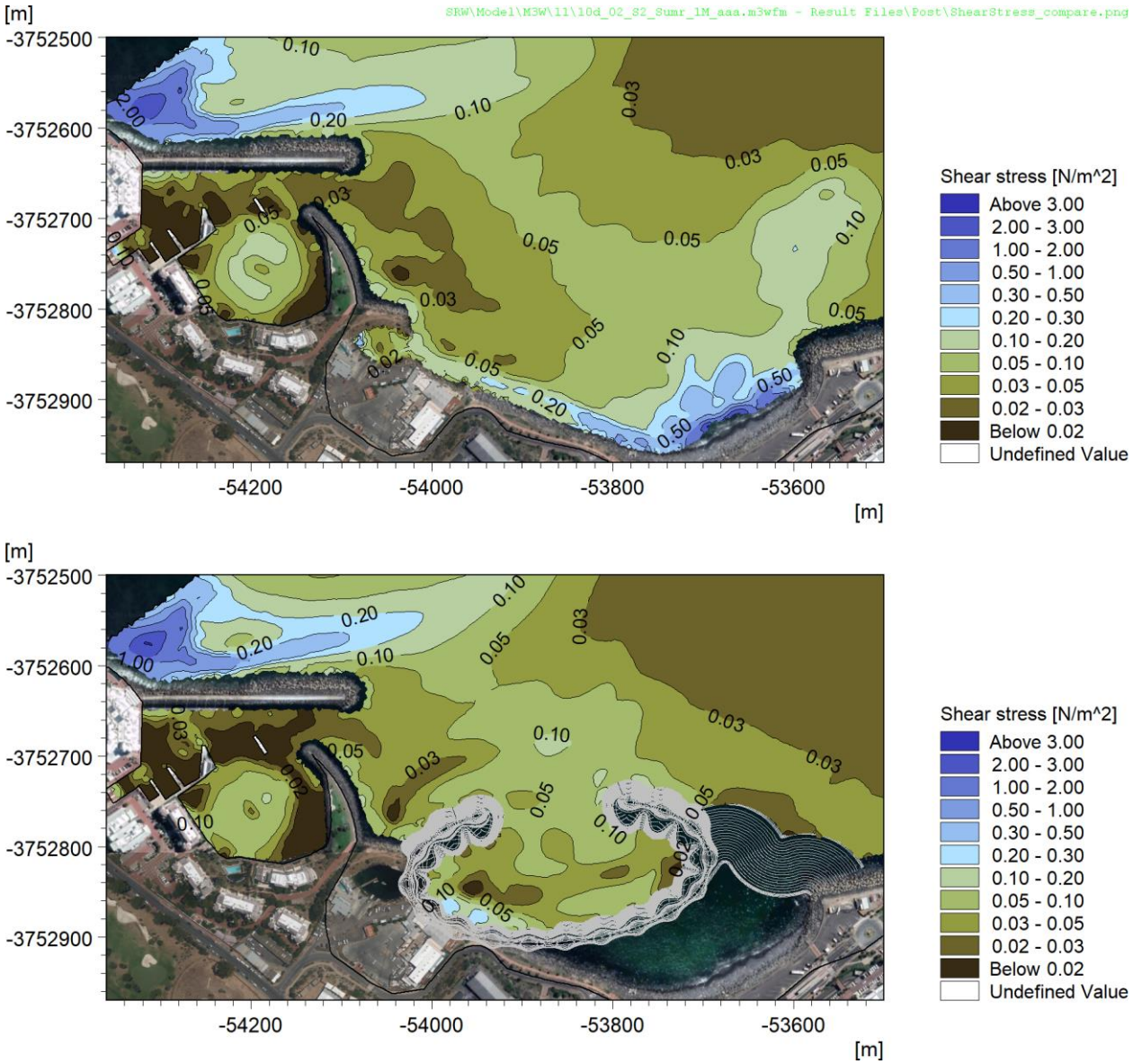

Figure 3-14: Wave-induced bed shear stress for baseline (top) and development (bottom) layouts for the 1-month return period storm event in summer.

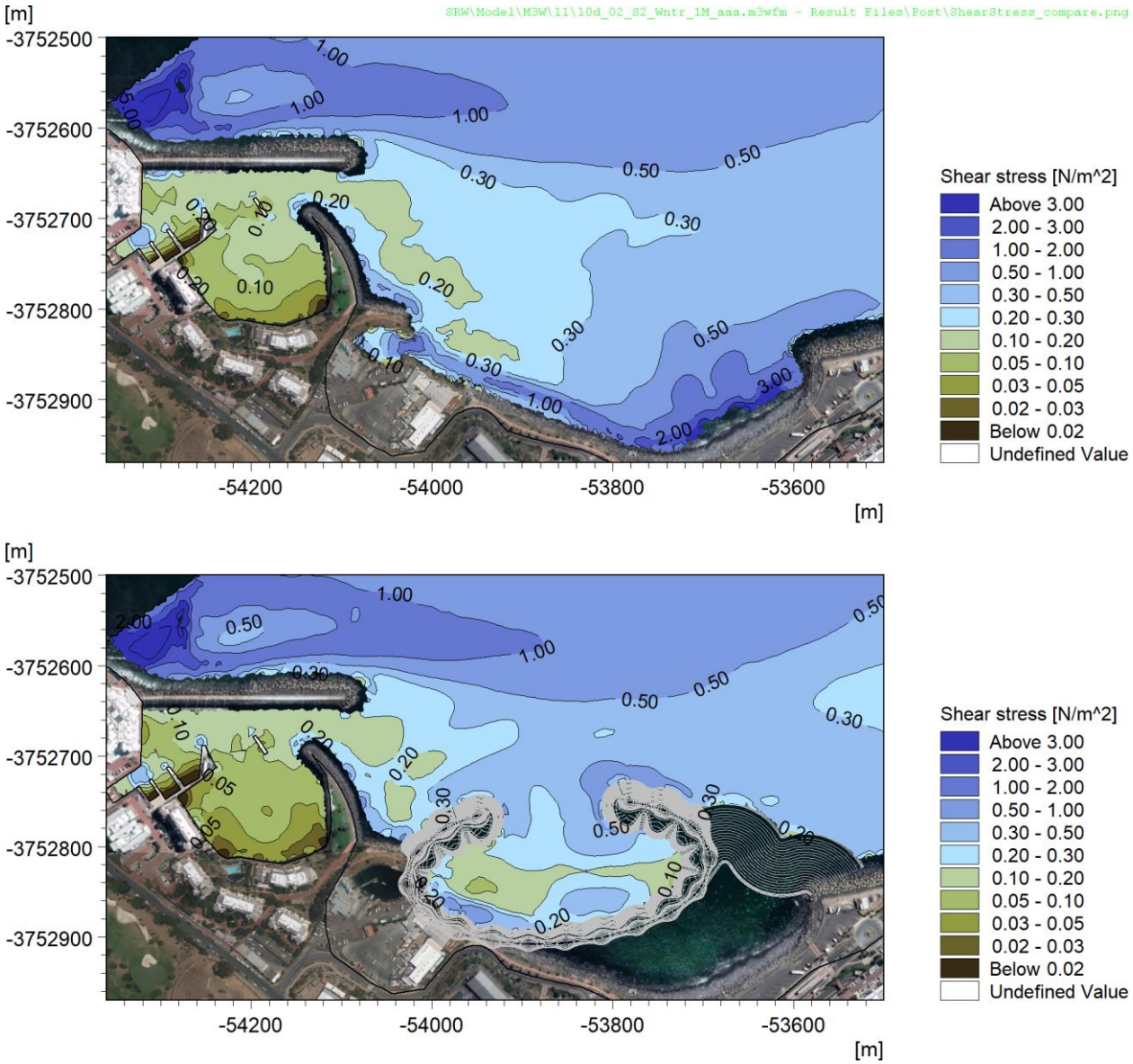

Figure 3-15: Wave-induced bed shear stress for baseline (top) and development (bottom) layouts for the 1-month return period storm event in winter.

The figures above show that:

- For the baseline case, mud will accumulate on the seabed in the area of the development during summer, but this will mostly be resuspended in winter and completely resuspended once a year, thus no longer-term accumulation of mud will occur on the seabed.
- For the development case, mud will accumulate on the seabed within the development during summer, with approximately half of the development seabed area remaining muddy after winter and two small areas remaining muddy after one year. There is thus some risk of longer-term mud accumulation within the development.
- For the baseline case, longer-term mud accumulation is predicted within the entire inner area of the Waterclub, except for the entrance and some localised areas of scour induced by strong currents due to harbour resonance. This result is consistent with bathymetric surveys of the Waterclub (see Figure 2-22) and historical dredge records, which indicate that periodic maintenance dredging of the Waterclub has been required.

- The development does not result in significant changes in mud accumulation beyond 300 m north of the development. The development has no significant impact on the bed shear stresses in the Waterclub, thus no additional mud accumulation and no additional volume of maintenance dredging is predicted for the Waterclub.

4. SUMMARY

The study used the existing situation as a baseline and compared the changes in currents, waves, sediment resuspension and temperature to assess impacts of the new development. The model results indicate the following:

- The addition of the development reduces the maximum current speed inside the development from 0.06 m/s in summer and 0.04 m/s in winter to 0.02 m/s.
- The maximum current speeds inside the new development are higher (0.02 m/s) than those inside the Waterclub (0.01 m/s).
- The residual circulation inside the new development comprises twin eddies which will induce flushing of water out of the development.
- The residual circulation is stronger in summer/autumn due to the strong south-east winds.
- The residual circulation within the development is slightly weaker than the baseline circulation, but stronger than the circulation within the Waterclub.
- The maximum surface seawater temperature inside the development area increases slightly (by about 0.25°C) in the winter/spring case, but remains the same in summer/autumn.
- The weaker residual circulation within the Waterclub results in a build-up in seawater temperature inside the Waterclub marina, particularly in summer.
- The wave height inside the development is generally reduced compared to the baseline layout, however there is significant amplification in the centre of the development due to harbour resonance.
- The wave height inside the development is significantly larger than those inside the Waterclub.
- For the baseline case, mud will accumulate on the seabed in the area of the development during summer, but this will mostly be resuspended in winter and completely resuspended once a year, thus no longer-term accumulation of mud will occur on the seabed.
- For the development case, mud will accumulate on the seabed within the development during summer, with approximately half of the development seabed area remaining muddy after winter and two small areas remaining muddy after one year. There is thus some risk of longer-term mud accumulation within the development.
- For the baseline case, longer-term mud accumulation is predicted within the entire inner area of the Waterclub, except for the entrance and some localised areas of scour induced by strong currents due to harbour resonance. This result is consistent with bathymetric surveys of the Waterclub and historical dredge records, which indicate that periodic maintenance dredging of the Waterclub has been required.
- The development does not result in significant changes in mud accumulation beyond 300 m north of the development. The development has no significant impact on the bed shear stresses in the Waterclub, thus no additional mud accumulation and no additional volume of maintenance dredging is predicted for the Waterclub.
- The development does not result in significant changes to currents or temperature beyond 300 m of the development, and beyond 500 m in the case of waves.

These model results will need to be interpreted by the marine ecologists to assess the impact on the marine ecology.

5. REFERENCES

DHI, 2023a. *MIKE by DHI Flow Flexible Mesh Model, User Guide,* Copehagen, Denmark: Danish Hydraulics Institute.

DHI, 2023b. *MIKE by DHI Flow Flexible Mesh, Scientific Documentation,* Copenhagen, Denmark: Danish Hydraulics Institute.

DHI, 2023c. *MIKE C-MAP, Extraction of World Wide Bathymetry Data and Tidal Information, User Guide,* Hørsholm, Denmark: Danish Hydraulics Institute.

DHI, 2023d. *MIKE 3, Waves FM Module, User Guide,* Copenhagen, Denmark: Danish Hydraulics Institute.

DHI, 2023e. *MIKE 3, Waves FM Module, Scientific Documentation,* Copenhagen, Denmark: Danish Hydraulics Institute.

DHI, 2023f. *MIKE 3, Wave Model FM. Validation Report,* Copenhagen, Denmark: Danish Hydraulics Institute.

DTU, 2010. *Improvement in global ocean tide model in shallow water regions,* Copenhagen, Denmark: Technical University of Denmark.

ECMWF, 2020. *European Centre for Medium-Range Weather Forecasts: ERA5.* [Online]
Available at: https://confluence.ecmwf.int/display/CKB/ERA5+data+documentation
[Accessed October 2020].

HYCOM, 2020. *Hybrid Coordinate Ocean Model.* [Online]
Available at: https://tds.hycom.org/thredds/catalogs/GLBy0.08/expt_93.0.html
[Accessed 2020].

PRDW, 2022. *Granger Bay Vision: Wave Modelling Report S2105-04-RP-CE-002-RA,* Cape Town: PRDW.

Tritan Survey, 2021. *The Water Club Granger Bay Bathymetric Out Survey: TS10180,* Cape Town: Tritan Survey.

Underwater Surveys, 2022. *V&A GRANGER BAY BATHYMETRIC SITE INVESTIGATION,* Cape Town: Underwater Surveys (Pty) Ltd.